OPTIMIZATION OF PARAMETERS AFFECTING ELECTROCHEMICAL PERFORMANCE OF CAPACITIVE DEIONIZATION CELL

Author:
Amro Mohammed Yahia Fadl
10663870

Supervisor:
Professor Antonello Vicenzo
Co-supervisor:
Maksim Bahdanchyk

Academic year 2020/2021

Abstract

Capacitive deionization (CDI) is an emerging technology for the removal of charged ionic species from aqueous solutions, that can be tailored for desalination applications. The technology utilities highly porous carbon materials as a pair of electrically charged electrodes, where ion electrosorption occurs at the electrical double layer (EDL) on the surface of the electrodes. The major strength points of CDI are its capability for selective ion electrosorption and energy efficiency. However, vast improvements are to be made to boost performance and stability, due to the complex interfacial chemistry of carbon-based materials. Therefore, this work tackles the problem of operational stability and performance optimization of a CDI lab-scale system. Activated Carbon (AC) electrodes are used for its high specific surface area and specific capacitance, in addition to relative stability and low cost. A flow-by CDI cell is used with various modifications to the structure by incorporating an anionic and cationic exchange membranes (AEM and CEM, respectively), leading to experimentation with CDI, AEM-CDI, CEM-CDI, and Membrane CDI (MCDI). First, the fundamental performance metrics of the process, namely salt adsorption capacity (SAC) and average salt adsorption rate (ASAR) show an inverse proportional relationship to flowrate of the aqueous sodium chloride solution (10 mM NaCl), over the range from 5 ml min^{-1} to 30 ml min^{-1}, though with an overall small change over this range. Secondly, cell preparation and assembly are optimized towards optimal desalination performance and operational stability. It is realized that by appropriate electrode pre-wetting, CDI cell tightening, and operating voltage less than 1.0 V, long-term operational stability and maximal SAC values can be obtained. Then, it is observed that faradic reactions are primarily responsible for pH fluctuations during operation and for the degradation of the AC electrodes; therefore, they are responsible for the impracticality of the CDI basic technology for water desalination applications. Therefore, in this work, electrochemical performance is optimized by realizing a

balance between flow rate, applied potential and cell assembly for the purposes of brackish water desalination.

Sommario

L a deionizzazione capacitiva (CDI) è una tecnologia emergente per la rimozione di specie ioniche cariche da soluzioni acquose, che attraversa una fase di continuo sviluppo tecnologico in vista della sua maturazoine a tecnica di desalinizzazione. Una cella CDI comprende due elettrodi di carbone attivo altamente porosi, così da garantire un'elevata capacit> di adsorbimento ionico entro il doppio strato elettrico (EDL) che si forma alla superficie degli elettrodi. I principali punti di forza del CDI sono la capacit> di elettrosorbimento selettivo di ioni e l'efficienza energetica. Tuttavia, per migliorare prestazioni e stabilit> operativa, è necessario uno studio dettagliato del processo, che rifletta la complessit> dei fenomeni di interfaccia dei materiali a base di carbonio. Preliminare a questo studio è la messa a punto di un sistema sperimentalmente affidabile e robusto e, a questo scopo, abbiamo intrapreso un lavoro di indagine sugli aspetti pratici ed operativi del processo di deionizzazone capacitiva utilizzando una cella e un sistema di monitaraggio realizzati in laboratorio. Questo lavoro affronta pertanto il problema della stabilit> operativa e dell'ottimizzazione delle prestazioni del sistema CDI realizzato in laboratorio. Si usano elettrodi di carbone attivo (AC) per la sua elevata area superficiale specifica e capacit> specifica, oltre alla relativa stabilit> e al basso costo. Viene usata una cella CDI a flusso sia nella configurazione base, con una coppia di elettrodi AC e separatore (cella CDI) sia in diverse configurazioni che includono una o due membrane a scambio ionico, portando alla sperimentazione delle celle con una singola membrana (AEM-CDI, con membrana anionica; CEM-CDI, con membrana cationica) e della cella con entrambe le membrane, MCDI. Innanzi tutto, i parametri di prestazione fondamentali del processo, vale a dire la capacit> di adsorbimento salino (SAC) e la velocit> media di adsorbimento salino mostrano una relazione inversa con la velocit> del flusso della soluzione (10 mM NaCl), nell'intervallo di velocit> di flusso da 5 ml min^{-1} a 30 ml min^{-1}. In secondo luogo, si è provveduto ad ottimizzare preparazione e assemblaggio della cella rispetto al comportamento nelle prove di dissalazione. Si è riscontrato, entro i limiti di questo lavoro sperimentale, che vi sono alcune misure di particolare importanza da adottare nell'allestimento del sistema sperimentale allo scopo di

conseguire stabilit> operative e massimizzare la capacit> di adsorbimento salini, quali un'attenta e appropriata pre-bagnatura degli eletrodo, l'adeguata chiusura della cella per un garantire le condizioni di flusso, una tensione di cella non superiore a 1 V. Le reazioni faradiche che hanno luogo durante l'adsorbimento sono responsabili di importanti fluttuazioni di pH durante il funzionamento della cella e della degradazione degli elettrodi di carbone attivo con il tempo di funzionamento; pertanto, esse sono anche responsabili dell'impraticabilit> della tecnica CDI nella sua forma base (senza impiego di membrane a scambio ionico) per quanto riguarda le applicazioni di desalinizzazione dell'acqua. Pertanto, in questo lavoro, si è ottimizzato il processo elettrochimico cercando un opportuno equilibrio tra potenziale applicato, velocit> di flusso e preparazione e allestimento della cella ai fini della desalinizzazione dell'acqua salmastra

Table of Contents

Chapter I

Introduction

Capactive deionisation is an emerging desalination technology with a superior selective ion adsorption and energy efficiency. It utilities porous carbon-based electrode materials for their high specific surface area and specific capacitance. Additionally, carbon materials are generally low cost and widely available, making it feasible for wide-spread adoption. Various innovations are being developped for CDI systems, with a growing research interest making way for novel cell architectures and electrode materials. The main phenomena responsible for the adsorption/desorption of charged ionic species is the electrical double layer, that exist at the interface between porous electrodes and electrolyte. Charging of the cell can occur with two modes: constant voltage or constant current, while the applied potential plays a vital role in the presence of parasitic reactions that affects negatively both energy efficiency and operational stability.

1.1 Water Consumption

The need for a reliable and continuous supply of fresh water remains a major component of life and human development. Over the millennia, fresh water supply has been plentiful in most areas of the world contributing to the enormous developments we see today. However, extracting extensive water from wells, lakes, and rivers for agricultural, industrial, and human needs put at risk health of aquatic ecosystems and increase water scarcity. It is estimated that 1.4 billion people live in regions that will

experience severe water scarcity within the first quarter of the century. By 2025, those regions will not be able to meet the 1990 levels of per capita food production from irrigated agriculture, neither the water needs for domestic, industrial, and environmental purposes [1].

It remains of great importance to reserve water for affected ecosystems while keeping up with the rate of population growth and the uncertainties of climate change. This can be achieved by focusing on a few major goals. The first would be a global effort to ensure that freshwater ecosystems receive adequate water quality and quantity to maintain its ecological functions. Secondly, to increase water productivity; getting twice as much service, satisfaction, and benefit out of each unit of water extracted from natural resources [2]. Finally, to develop an efficient and economic desalination technology to address portable water scarcity problem. These goals in conjunction could relieve the water stress on 2.1 billion people, keeping up with industrialization, population growth, climate change, and water contamination [3].

Boosting and securing a reliable supply of freshwater by seawater and brackish water desalination will act on both increasing water productivity and developing solutions to address portable water scarcity. Of the various desalination technologies developed, such as electrodialysis, distillation, and reverse osmosis (RO), infrastructure costs and the high energy requirements pose a significant challenge to the economic and environmental practicality of these technologies. Capacitive deionization (CDI) is an emerging electrochemical desalination technology that continues to attract research interest worldwide for its potential energy saving and environmentally friendly application. However, the technology has significant challenges in terms of performance degradation and inefficiency at higher salinity feeds that affects its practicality. Therefore, various cell architectures, electrode materials, and operating parameters are developed and optimized to boost performance and operational longevity [4].

1.2   Conventional Water Desalination Technologies

Membrane technologies rely on the presence of semi-permeable membranes in a water purification system with varying pore size and ion selectivity. The three main driving forces for membrane filtration are electricity, pressure and temperature as shown in

Figure 1.1a. Usually, membranes are a thin film of porous material that potentially block, roughly speaking, particles and/or molecules of size larger molecules than its pore size, ranging from ionic and molecular species to viruses, bacteria, and suspended solids. The membrane materials can be a variety of polymeric materials such as nylon, acetate, and cellulose, or non-polymeric materials such as ceramics, metals, and composites [5]. A wide range of filtration processes are pressure driven, which is the case for Reverse Osmosis (RO), Nanofiltration (NF), Ultrafiltration (UF), and Microfiltration (MF), or electrically driven such as electrodialysis (ED) or electrodialysis reversal (EDR) [5].
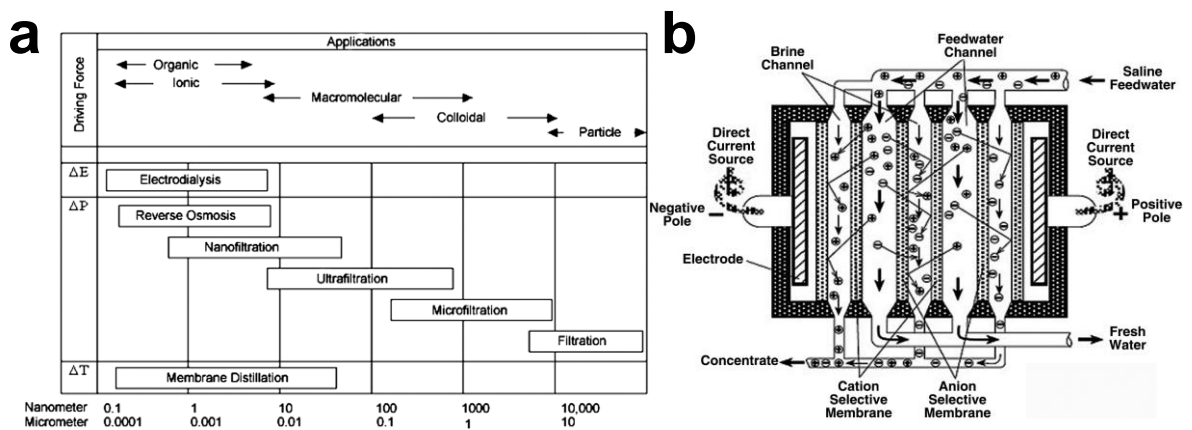

Figure 1.1. a) Effective range of membrane applications and b) scheme of ED cell [6].

Use of pressure driven membrane systems is a conventional way of a straightforward water purification. It utilizes pressure difference across the semi-permeable membrane as a driving force for water purification. The water to be treated is separated into a stream of filtrate and retentate, where the filtrate contains purified water stream while the retentate contains components rejected by the membranes. These membranes are well-defined barriers, allowing for continuous and reproducible control of the quality of filtrate independent from variations in the concentration of components in the feed stream. Plants operating with Microfiltration, Ultrafiltration, Nanofiltration, or RO membranes show high operating stability, high reflexivity, long term operational and economic reliability [7].

Microfiltration is the least restrictive membrane filtration process, with a pore size ranging from 0.1-1.0 µm and an operating pressure up to 5 bar. It eliminates bacteria, pigments, and other particulates with a size in the submicron range. Then comes

Ultrafiltration that, with an average pore size of 0.05 µm and an operating pressure up to 10 bar, further removes viruses, macromolecules such as sugars and proteins, and particles with a size range 0.01-0.1 µm. A different mechanism is used for Nanofiltration, where monovalent ions diffuse through the membranes rather than being blocked from passing due to the membrane pore size. The operating pressure of NF can reach up to 10 bars and it further removes color, hardness, sulfates, and synthetic organic contaminants [5].

Reverse Osmosis operates with the tightest type of membranes available, where the organic and inorganic molecules are separated from the feed solution by a solution diffusion process. RO is used to separate dissolved salts with a molecular weight less than 200 gmol^{-1}. It is mostly used for desalination of sea water for drinking purposes and ultra-pure water for semiconductor or pharmaceutical uses as it is effective for removing total dissolved salt (TDS) concentrations of up to 45000 mgL^{-1}. However, RO requires high enough energy supply for the pump to raise the pressure applied to feedwater in proportionality to its TDS concentration. The pump pressure requirement is between 10 to 30 bar for brackish water and around 85 bar for seawater. This makes it a very energy intensive desalination technology [5,7].

On the other hand, Electrodialysis (ED) is an electrically driven process that has a high rate of water recovery, mainly used for wastewater treatment and brackish water desalination. The method does not involve phase change nor chemical additives making it a more environmentally friendly water treatment technique. ED mechanism involves a voltage applied between the cathode and anode electrodes, passing through ion exchange membranes (IEMs) that separates charged ions from uncharged matter and the aqueous solution, where the movement of ions inside of ED device is represented in Figure 1.1b. Normally, inside the ED stack, there are multiple anion exchange membranes (AEMs) and cation exchange membranes (CEMs) that are placed between the cathode and anode electrodes. The main function of the membranes is work as a selective barrier to nutrients and salts migration, based on their electrical charge. Then, when the feed enters the ED stack, the applied electrical potential on the electrodes leads to a reduction reaction at the cathode and an oxidation reaction at the anode. To illustrate, cationic species like Na^+, NH_4^+, and K^+ pass through the CEM and towards the cathode, while anionic components like CL^-, PO_4^-, and SO_4^- pass towards the anode through AEM [8].

1.3   Capacitive Deionization

Selective ion extraction from aqueous solution is a later step in the water purification and resource recovery fields. Capacitive deionization (CDI) is an emerging desalination technology, with an edge for regulating the ion electrosorption process and thus selective adsorption of target contaminants. CDI utilities porous electrodes to remove ionic species from aqueous solution when the cell is charged with an electrical potential, normally in the range 0.8 – 1.2 V, though commercial units can operate at higher cell voltage, typically below 1.8 V. Flow-by, flow-through, and flow electrode CDI are the main configurations for the technology, with the latter being a relatively new development. CDI performance can be drastically improved by utilizing modifications to the system. To illustrate, by applying ion exchange membranes between both electrodes, co-ions' adsorption could be prevented thus improving charge efficiency [9]. CDI was developed in the 1960s, with various architectures emerging as research interest grows in the field. Figure 1.2a represents the growing research interest by number of publications, while Figure 1.2b shows the timeline of development from the 1960 to 2019 [10].
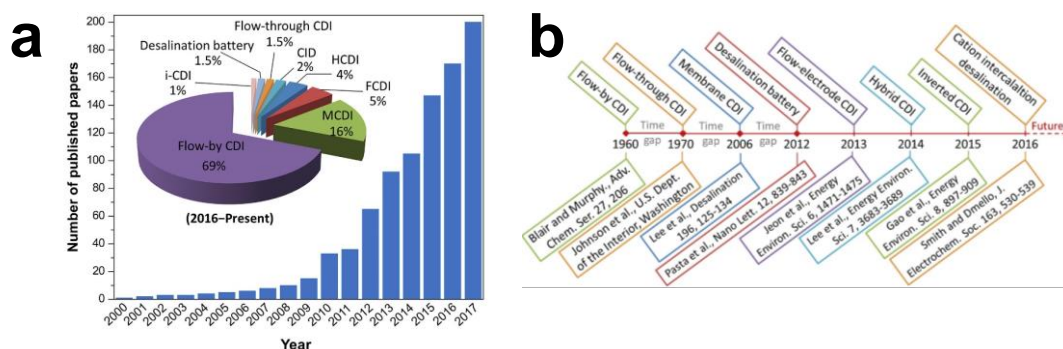

Figure 1.2. a) Evolution of the number of publications concerning CDI alongside pie graph exhibiting the percentage of the scientific reports of various CDI cell architectures, (b) timeline displaying the years when various CDI cell architectures emerged and the corresponding seminal work [10].

1.3.1   Theoretical Background

Regular CDI operation is a set of adsorption / desorption cycles, also known as charge/discharge or desalination/salination, achieved by application of external potential or current. Schematically, CDI consists of two electrodes with salt containing

electrolyte flowing in between as shown in Figure 1.3a. During charging external potential is applied and ions migrate to the oppositely charged electrodes, where they are stored as charge, as shown in Figure 1.3b. During discharge or regeneration step, the stored ions are released back to the feed solution as shown in Figure 1.3c. CDI working mechanism relies on the electrosorption of ions, which has a well-established theoretical basis. The major phenomenon beneath working principle of CDI unit is electrical double layer (EDL).
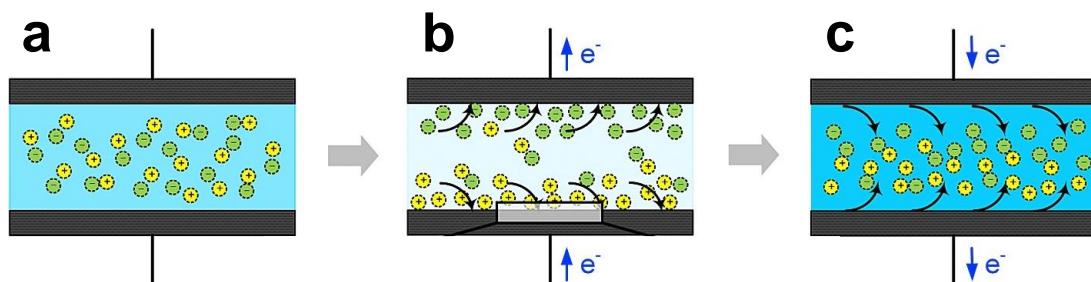
Figure 1.3. Single desalination/regeneration cycle in CDI [11].

Electrical double layer (EDL) forms when charged electrode is immersed in a solution with ionic species. The interface of the charged electrode will be occupied with counter-ions due to the electrostatic force. Stern adsorption model has been widely used to explain the experimental results as well as investigate the CDI process. Stern model of double layer structure explains the interfacial properties and structure between an electrode (electronic conductor) and an aqueous electrolyte (ionic conductor). The model states that the double layer can be divided into a compact and a diffusion region. The inner dense region, also named Helmholtz layer shown on Figure 1.4a, has ions adsorbed in molecular closeness to the surface of the electrode, forming ideally a planar layer of charged particles. Whereas the diffusion region, called Gouy-Chapman layer (Figure 1.4b), has a distribution of electric charge dependent on the distance from the surface and the electrolyte concentration. Figure 1.4c shows a schematic representation of the Stern's EDL structure.
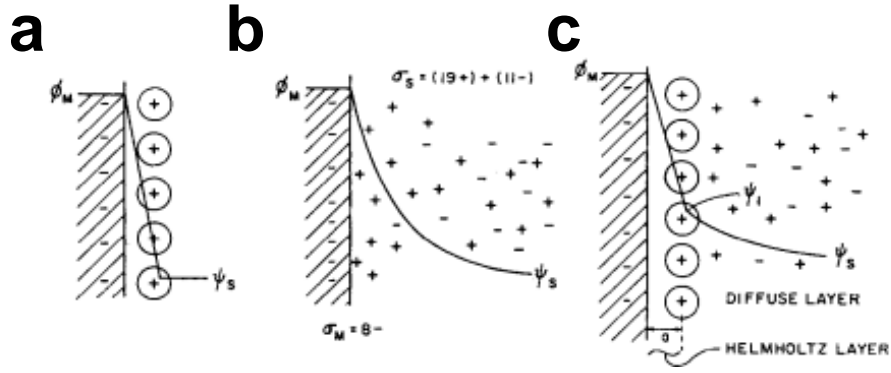
Figure 1.4. Evolution of EDL theory a) Helmholtz model, b) Gouy-Chapman and c) Stern model [12].

Both capacitances of the two layers contribute to the total capacitance, thus the total capacitance can be calculated as a series combination of the inner Helmholtz layer and the diffusive Gouy-Chapman layer, expressed in Equation (1.1)

$$\frac{1}{C_T} = \frac{1}{C_H} + \frac{1}{C_{GC}}$$

(1.1)

where: C_T is the total capacitance, C_H is the capacity of the inner compact layer, and C_{GC} is the capacity of the Gouy-Chapman layer.

Helmholtz compact layer usually is explained as a classic parallel-plate capacitor, where charge separation is electrostatic, and the capacitance is directly proportional to the area of the plates and inversely proportional to the distance of separation according to Equation (1.2).

$$C_H = \varepsilon_r \varepsilon_0 \frac{A}{D}$$

(1.2)

Where C_H is the capacitance in F, A is the area of each plate in m^2, ε_r is the relative electrostatic permittivity or dielectric constant of the medium between the plates, ε_0 is the permittivity of free space (8.854×10^{-12} Fm^{-1}), and D is the separation between the plates in m.

According to the Gouy-Champan model, the capacitance of the interface is related to the potential drop across the EDL and to the ionic concentration of the electrolyte according to Equation (1.3)

$$C_{GC} = 228z\sqrt{C}cosh(19.5z\phi_0) \tag{1.3}$$

where z is the charge number of the ion, C is the bulk ion concentration, and ϕ_0 is the potential drop across the diffuse layer.

In practical CDI processes, both C_H and C_{H-S}, contribute to the total capacitance, therefore to achieve high adsorption capacity, the main focus shall be on increasing the specific surface area of the electrodes [13].

1.3.2 Electrode Materials

Performance of CDI unit is strongly related to electrode material properties such as specific surface area, electrical conductivity, hydrophilicity, and electrochemical stability. For that, the most widely used electrodes in CDI applications are carbon-based electrodes, many of which have high electrical conductivity, low contact resistance, appropriate wetting behavior, good processability, desirable bio-inertness, low cost, and chemical stability. Various forms of carbon including its allotropes and composites are used such as activated carbon, carbon cloth, carbon aerogel, carbon nanotubes, carbide derived carbons, and graphene. Those materials are ideal for electrosorption as they have high specific surface area and porous structures , as shown in Figure 1.5 thus their advantage for CDI application [14].
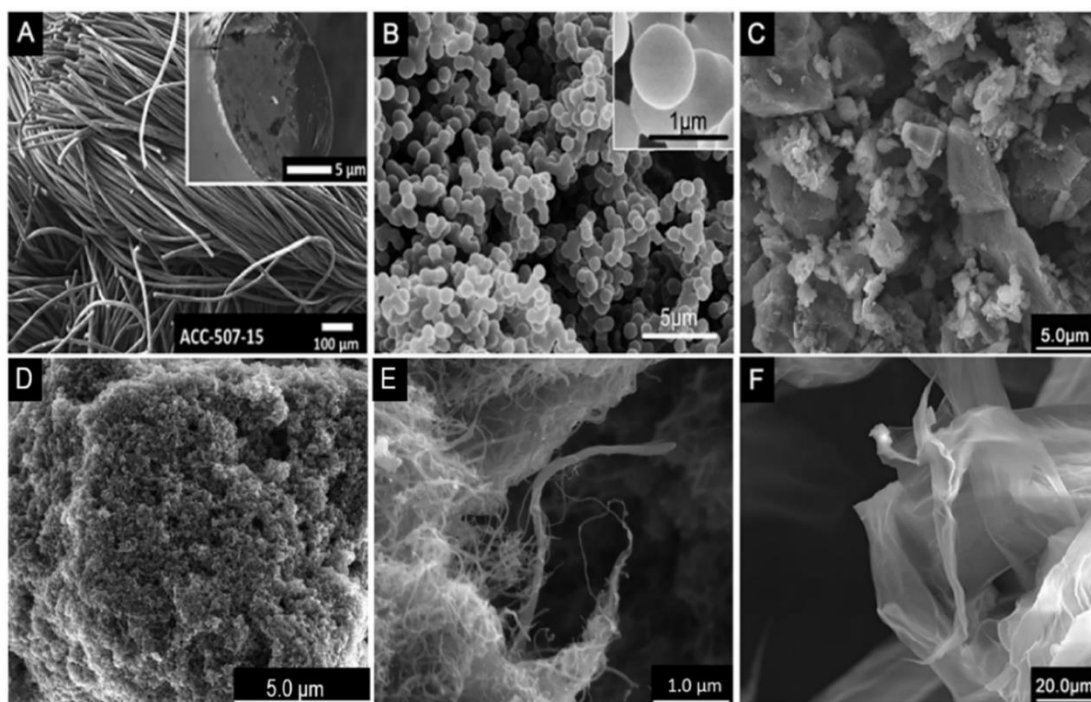
Figure 1.5. Morphologies of different carbon materials used in CDI electrodes. a) Activated carbon cloth (ACC) produced with CNF, b) carbon spheres, c) activated carbon, d) carbon black, e) Carbon Nanotubes, and f) Graphene [15].

Activated carbon (AC) is currently the most widely used for water purification when it comes to adsorption-based purification techniques. It is characterized as a carbonaceous material with a highly porous internal structure with a range of pore size, from macro (> 50 nm), to meso (2-50 nm), and micro (< 2nm) pores, all present in its highly branched internal structure. The presence of these pores is mainly responsible for the advantageous high specific surface area, of up to 2500 m^2g^{-1}, allowing for a large number of binding sites for adsorbate species. However, the actual pore structure and internal composition is determined by the source material, the activation process, and further chemical modifications, as AC can be derived from the pyrolysis and chemical treatment of different sources, such as coal, wood, nutshells, bamboo, and other organic materials [16].

For CDI, the main advantages of using AC as electrode material is the high specific surface area, simple preparation, and low production cost. Therefore, it possible to attain economically feasible desalination. The electrodes are usually prepared using a conductive agent and a binder, whose function is to improve the adhesion of AC powder and increase the electrical conductivity. However, as the conductive agent and binders hardly contribute to the CDI capacity, free-standing AC electrodes were proposed to increase the active material load. Furthermore, surface modifications of AC with

various oxygen containing functional surface groups can improves the CDI performance by improving the hydrophilicity and deionization capacitance [4]. Alternatively, the application of single-walled carbon nanotubes (SWCNTs), double-walled carbon nanotubes (DWCNTs), as well as multi-walled CNTs as electrodes for removing various hazardous ions from brackish water has been widely researched in the last years. Also graphene, which is a two dimensional sp^2 hybridized monolayer of carbons sparked a great attention for its physical and chemical properties. For CDI application, graphene shows high electrosorption capacity whereas CNTs are used for its high aspect ratio and surface area, as well as its exceptional electrical properties. As an example of the use of such materials for fabrication of CDI electrodes [17], a CNT electrode showed a network structure with a specific surface area of 415 and 453 m^2g^{-1} for DWCNTs and SWCNTs respectively, while the graphene electrode had a layered structure with extensive smooth surface, and a low SSA of 77 m^2g^{-1}.

For CDI, the kinetic electrosorption studies demonstrate that CNT samples are superior to graphene by simulating the values of free energy of adsorption (ΔG_0) in accordance with Langmuir and Freundlich isotherms. The experimental data observed ΔG_0 values of -16.73, -17.82, and -17.93 kJmol^{-1} for DWCNT, SWCNT, and graphene respectively. The more negative the ΔG_0 value is, the greater is driving force of electrosorption and thus the higher electrosorptive capacity. However, other factors also contribute to CDI electrode efficiency such as pore structure and hydrophilicity. As graphene has lower hydrophilicity and smaller SSA than other carbon nanomaterial electrodes, the adsorption capacity of CNTs was larger in comparison with graphene as shown in Figure 1.6 [15].
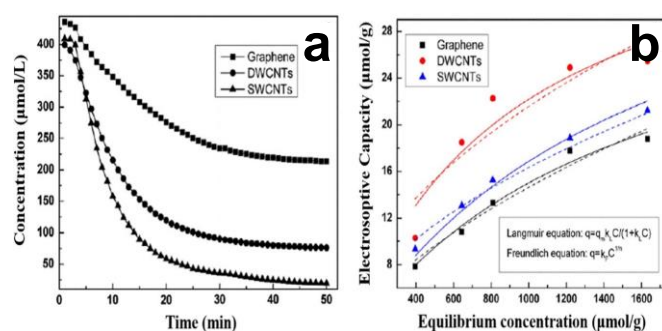

Figure 1.6. a) Variation of NaCl concentration with time for CDI at 2.0 V, b) Experimental and modelled data with solid line referring to Langmuir model while dashed line referring to Freundlich model [15].

10

1.3.3 Cell Architectures

A conventional CDI cell consists of two current collectors facilitating electron transfer between the electric contacts and the electrodes, two electrochemically active materials for capacitive ion sorption, a spacer channel for the feed water to be transported in, and a mesh separator between the electrodes to prevent short-circuit. For Flow-by CDI, the feed water flows between the electrodes while for Flow-through CDI the feed water flows through the electrodes as shown in Figure 1.7a, c respectively

Upon applying a potential difference across both electrodes, cations (e.g. Na^+, K^+) in the spacer channel are electrostatically attracted to the negatively charged electrode and anions (e.g. Cl^-) are attracted to the positively charged electrode. The potential difference applied between the electrodes is limited by the thermodynamic stability of water, $E_0 = 1.23$ V_{SHE} [13]. Overcoming this limit leads to the progressive loss in the cell performance related to appearance of unwanted faradic reactions (e.g., water oxidation). This charging, or adsorption, step generates the purified water stream. On the contrary, following ion-adsorption, electrodes can be regenerated by reversing the polarity or short-circuiting the positive and negative electrode. This discharge or desorption step releases ions back into the bulk solution generating a stream of concentrate. Therefore, purified water and brine streams are produced intermittently.

Membrane capacitive deionization (MCDI) is a significant improvement over conventional CDI, and it involves the inclusion of ion exchange membranes (IEMs) in front of the electrodes as shown in Figure 1.7b. Cation exchange membrane (CEM) is placed adjacent to the negative electrode and an anion exchange membrane (AEM) is placed adjacent to the positive electrode. The major benefit of IEMs is that counter-ions are unable to penetrate the membranes when they are expelled from the micropores and therefore stay in the macropores of the electrode during the charging step. Since the macro-pores are electrically neutral, they could serve as extra storage space for counter-ions, thereby improving the ion adsorption capacity or removal performance. Another significant benefit of IEMs is the extension of the life time of electrodes as it helps with alleviating some faradic reactions and avoids direct water scouring [10].
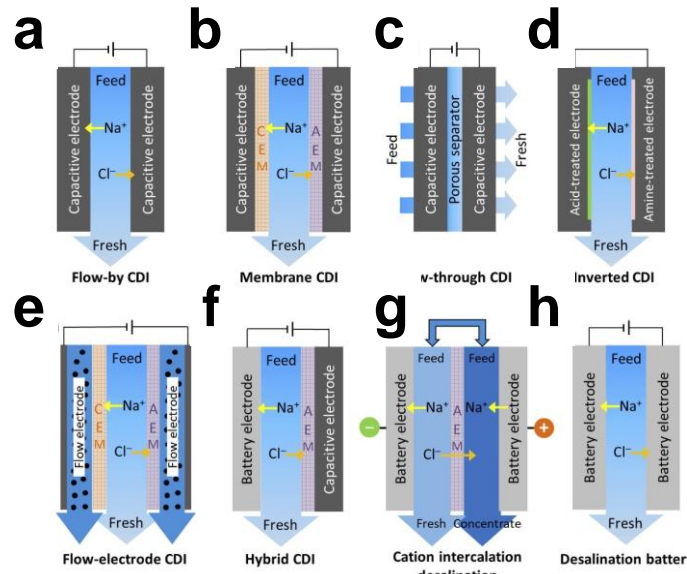
Figure 1.7. Various CDI cell architectures: a) flow-by CDI, b) membrane CDI, c) flow-through CDI, d) inverted CDI, e) flow-electrode CDI, f) hybrid CDI, g) cation intercalation desalination, and h) desalination battery [10].

Even though flow-by CDI and flow-through CDI are the most utilized cell architecture, especially with IEMs, various novel CDI cell architectures found their proliferation in the recent years. Inverted capacitive deionization (i-CDI) is shown in the Figure 1.7d. It results from a modification of a flow-by CDI by using a positive electrode with a net negative surface charge and a negative electrode with a net positive surface charge. This structure is responsible for its inverted adsorption-desorption behavior, where ion desorption occurs during the charging step and ion adsorption occurs during the short-circuit or cell discharge. i-CDI exhibits a dramatic increase of performance stability and lifetime in comparison to CDI under the same operating conditions, due to the mitigation of parasitic faradic reactions, especially carbon oxidation at the anode [10]. Flow-electrode CDI (FCDI) is another cell architecture that arose from a modification of MCDI, where fixed electrodes between IEMs and current collectors are replaced with flowing electrodes made of carbon suspension as shown in Figure 1.7e. This enables continuous ion removal and steady state production of desalted water, that can be of high salinity, as electrode regeneration is completed downstream of the cell by mixing positive and negative carbon slurries followed by carbon separation from water via setting.

Owing to the superior ion sorption capacity of battery electrodes in comparison with traditional capacitive electrodes; hybrid CDI (HCDI), cation intercalation desalination (CID), and desalination battery Figure 1.7f,g,h are receiving increased attention. These

cells operate using reversible redox reactions or the mechanism of faradaic processes. Generally, HCDI cell consists of a faradic electrode for cation adsorption/desorption and a capacitive electrode for anion adsorption/desorption, with AEM placed adjacent to the capacitive electrode to enhance its performance. As for the desalination battery, it is composed of two battery/faradic electrodes responsible for the adsorption/desorption of cations and anions present in the solution. Finally, CID cell is maintained by employing faradaic cation intercalation materials for both electrodes separated by an AEM.

1.3.4 Operation Modes

CDI technology utilizes a cyclic method of water desalination where salt ions are removed during the charging step and released again during the discharge after being temporarily held in the pores of the electrodes. During charging, an input of electrical energy is needed throughout the step which can be partially recovered during discharge. Two charging modes are used based on the power supplied to the CDI system: Constant voltage (CV) and constant current (CC). Both modes have different desalination responses, system requirements, and energy efficiency [18]. Upon applying constant voltage on the cell, a spike in current measurement is observed at the instant of induced potential difference, followed by exponential relaxation to near zero levels as shown in Figure 1.8a. Alternatively, by supplying a constant current, voltage increases linearly throughout the duration of the experiment as shown in Figure 1.8b.
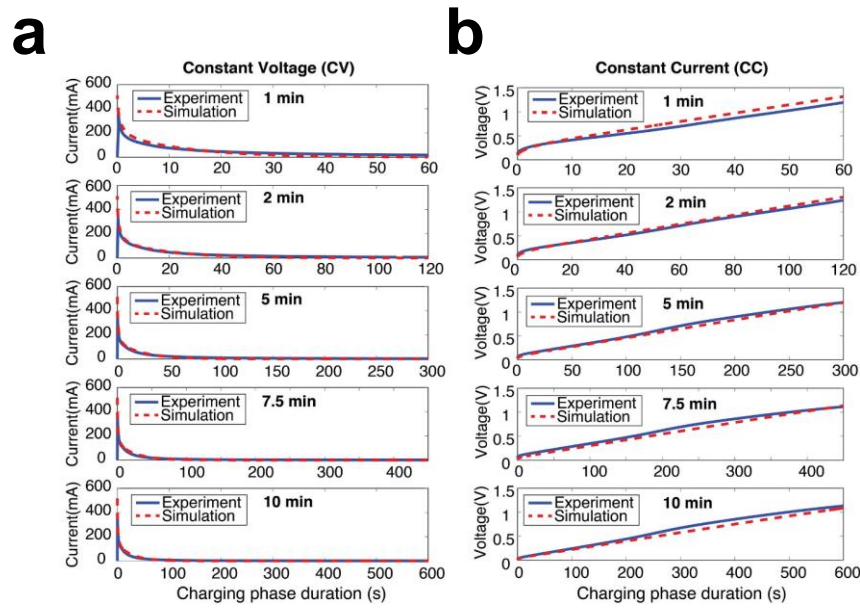
Figure 1.8. Experimental and simulated response of CDI cell with charging phase durations of 1, 2, 5, 7.5 and 10 minutes (a) current response under constant voltage operation of 1V and (b) voltage response under constant current operation [11].

Theoretical and experimental studies prove that CV mode consumes significantly more energy than CC mode (around 50% more energy consumption). In addition, around 5.7% of the total energy consumption during charging process in CV mode can be recovered in comparison with 40% recovery for CC mode. This CC mode superiority in terms of energy efficiency can be explained in terms of energy dissipation. Fundamentally, energy dissipates in the form of heat as current pass-through resistances. As CC mode has better control of charging currents, the CDI cell dissipates less power through resistive components. Another advantage of CC is that it reduces the time of operation where the electrode-to-solution potentials result in parasitic reactions, therefore improving energy efficiency. However, energy consumption is different from energy input to the cell as only a fraction of the energy input is dissipated or consumed by the cell, while the other fraction is stored within the cell as capacitive energy in the electrical double layer. This stored energy is recoverable and not consumed by the cell. Therefore, under low current discharge, energy dissipated by resistances and parasitic reactions are minor compared to recoverable electrical capacitance, which can be used to charge other CDI cells or stored externally [19].

1.3.5 Performance Metrics

To measure the effectiveness of CDI in terms of desalination ability and energy efficiency, key performance metrics are used to make possible comparisons between different experiments and setups, acting as an insightful indicator of CDI performance. However, it is important to distinguish between cell and electrode performance using a variety of metrics such as salt adsorption capacity, average salt adsorption rate, Kim-Yoon diagram for salt adsorption rate vs. capacity, charge storage capacity, charge efficiency and current efficiency [20].

A growing trend in CDI is to report the salt adsorption capacity (SAC) of the charge-discharge cycle, which can have any duration, from a short one with little adsorption, to sufficiently long where equilibrium adsorption is reached. The latter measures the maximum salt adsorption capacity (mSAC) or equilibrium salt adsorption capacity (eqSAC), which is a property of only the electrodes and should not be affected by other cell components, making it an insightful metric into CDI electrode sorption performance. To get to this equilibrium, fixed cell voltage must be applied and maintained until the charging step is complete and salt concentration is constant throughout the cell. This condition is indicated by the levelling to a constant value of the measured conductivity of the cell effluent.

Salt removed from water is then calculated according to Equation (**1.4**) by a time integral of the difference between cell inflow and effluent concentration multiplied by the flowrate through the cell, measured from the start of the charge until equilibrium is reached.

$$m_{salt} = V M_w \int_{t_0}^{t_1} \Delta C \ dt \qquad (1.4)$$

where $t_1 - t_0$ is charging/discharging time in s, ΔC is the change in salt concentration, M_w is the molecular weight of salt, in M, V is the flowrate measured in Ls^{-1} and m_{salt} is salt adsorbed measured in mg.

Since the amount of salt adsorbed is a parameter that depends on the electrode mass in CDI cell, the main metric used in the field is Salt Adsorption Capacity (SAC) and can

be estimated according to Equation (**1.5**) by dividing the mass of salt removed by the mass of both positive and negative electrode:

$$SAC = \frac{m_{salt}}{m_{el}} \tag{1.5}$$

Where SAC is measured in $mg\,g^{-1}$. Typically, the dry mass of all components of the electrode paste (porous carbon, binder, and other additives) are used in this calculation.

As SAC gives a sense of the amount of salt sorption by CDI electrodes, average salt adsorption rate (ASAR) gives information on the rate of salt sorption, and it is calculated according to Equation (**1.6**):

$$ASAR = \frac{SAC}{\Delta t} \tag{1.6}$$

Where *ASAR* is measured in mg g^{-1} min^{-1} and $\Delta t = t_1 - t_0$ refers to the charging time.

Several operational parameters can affect measured ASAR such as the charging time interval. Shorter charging times, especially in constant voltage operation, allow for much higher ASAR values as equilibrium adsorption might have not been reached. In addition, operating the cell at higher electrolyte salinity will yield faster charging and thus higher ASAR. Average salt adsorption rate is also dependent on cell architecture, where flow-through yields higher values than flow-by since flow-through minimizes the gap width between electrodes. In addition, electrode materials affect ASAR in many ways. For instance, sub-nanometer micropores allow for higher salt sorption but suffer from kinetic limitations associated with pore size, slowing down ion adsorption dynamics and therefore depressing ASAR. In addition, electrode thickness has an inverse proportionality to ASAR values, where thinner electrodes exhibit higher desalination rate capability. Also, the effect of cell compression, electrode thickness, and electrode microporosity are coupled together affecting ASAR in a complex way. Finally, combining both ASAR and SAC in one representation can give valuable insight as it allows for a clear determination of optimal cell operating conditions as shown in Figure 1.9a [20].
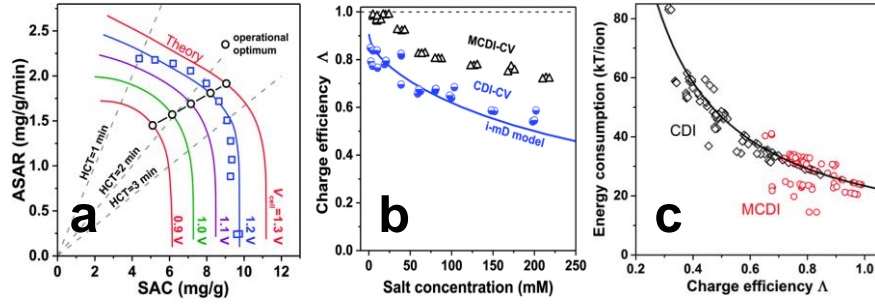
Figure 1.9. a) Ragone plot at different charging voltages, b) Charge efficiency as a function of salt concentration and c) energy consumption per ion removed vs. charge efficiency [20].

Charge storage capacity is a metric shared with the supercapacitor community that is obtained from the measured current as a function of time during charging and discharging steps. By integrating the current with respect to time, the electric charge (in Coulombs) transferred between the electrodes of the cell is obtained. Then by subtracting the leakage (non-capacitive) current, the calculated capacitive charge can be converted to (average) specific cell capacitance in Fg^{-1}, dividing by the applied cell potential and the total mass of the electrodes [20].

Charge efficiency, Λ, is the metric that describes the moles of salt removed per mole of electrons transferred between electrodes and is obtained by following Equation (1.7):

$$\Lambda = \frac{VF \int \Delta C dt}{\int I dt} \qquad (1.7)$$

where F is Faraday's constant (96485 C mol^{-1}) and $\int \boldsymbol{I dt}$ is the integral of the cell current during charging.

This value can then be compared to the measured salt adsorption rate per cycle. Charge efficiency is used in the analysis of static electrode CDI cycles as an integral property of the entire cycle and is a function of the cell voltage during charging and discharging as well as feed water salt concentration. Generally, Λ increases with higher charging and discharging voltages and with decreasing feed salt concentration as shown in Figure 1.9b. Also, it evaluates the electrical energy requirements of a CDI cell determining energy consumption as shown in Figure 1.9c [20].

1.4 Degradation Phenomena

Faradaic reactions have a direct and complex impact on the long-term performance of CDI cells. It is observed that the behavior of the electrodes and the CDI system changes alongside repeated charge-discharge cycling. In an experiment that studies this phenomenon on a flow-through and flow-by CDI cells, with AC electrodes, the appearance of inversion peaks was observed after 5 days of cycling for the flow-through cell compared to after about 18 days for the flow-by CDI cell [21]. The degrading trend of the latter cell is shown in Figure 1.10, where plots of salinity in ppm of NaCl vs. time/day during prolonged cycling of the flow-by CDI cell are shown. The overall testing time was 21 days, at cell potential of 0–0.9 V. Figure 1.10(A) shows the charge discharge cycling during the first day, (B) within the 10th day, (C) within the 18th day, and (D) up to the 21st day which marks the end of the experiment [21]. Normally, CDI cells are monitored by continuous electrolyte conductivity measurements at the outlet of the cell. When the CDI cell is polarized, electro-adsorption leading to removal of salt from affluent is expected, and therefore can be reflected by decreased solution conductivity at the cell outlet. On the contrary, when the cell is discharged through short-circuit or reversed polarization, an increase of salt concentration is expected and therefore an increase in electrolyte conductivity. This is the expected behavior and corresponds to the behavior revealed in the concentration profiles of Figure 1.10(A). The inversion effect is reflected by a desorption of ions into the bulk solution when the cell is being polarized and charged, while the solution shows signs of ion depletion through decreasing conductivity during the discharge of CDI cell.
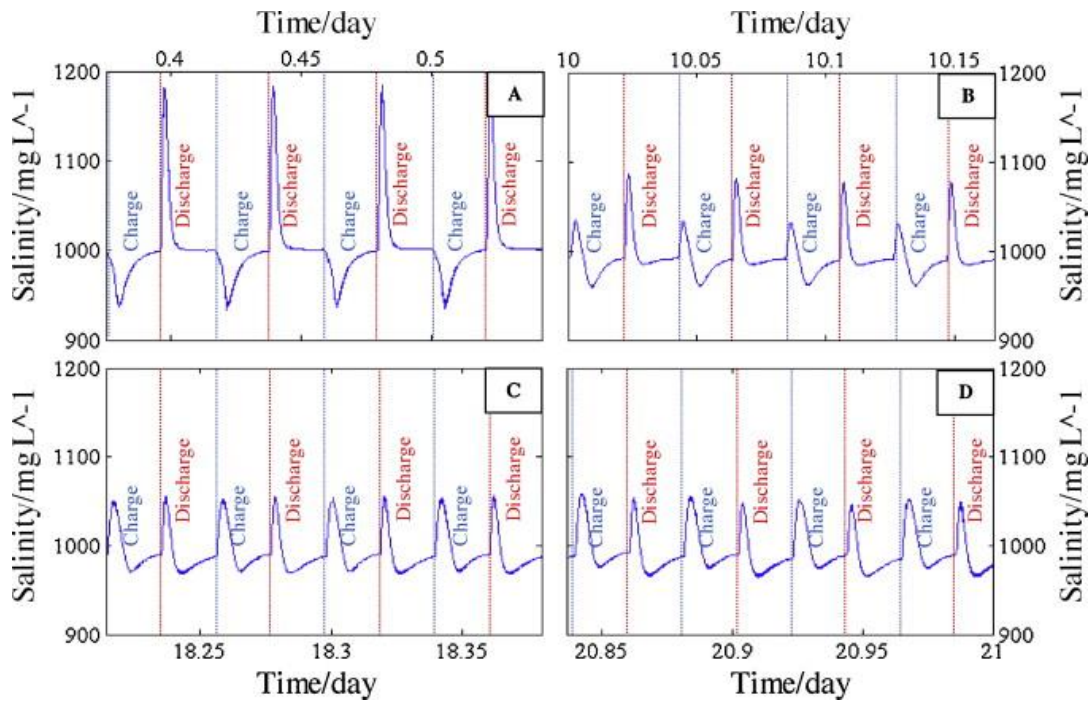
Figure 1.10. Desalination experiment in a flow-by CDI cell with ACC electrode, operated at 0.9 V / 0 V during charging and regeneration phase, respectively, revealing the inversion phenomenon. The four plots relate to selected significant time domains. The relevant potential application (charge/discharge) vs. time is marked [21].

The inversion effect can be explained by the oxidation of the anode in symmetric carbon-electrode CDI cells. As the anode is gradually oxidized and its pore structure damaged, the symmetry between the positive and negative counterparts are lost, leading to an unequally divided potential applied to both electrodes. The higher the oxidation level of the anode, the less symmetric the distribution of potential between the electrodes, the higher the potential falling on the anode further oxidizing it. Therefore, a way to limit this phenomenon is the reduction of the CDI operating potential to minimize the effects of anode oxidation. However, low applied potential means lower desalination capacity. The extent of electrode oxidation can be observed with respect to its resistivity increase, surface area decrease, and potential of zero charge (PZC) positive shift during prolonged operation. The physical effects can be visible on the carbon structure after prolonged CDI operation as shown in Figure 1.11 [21] .
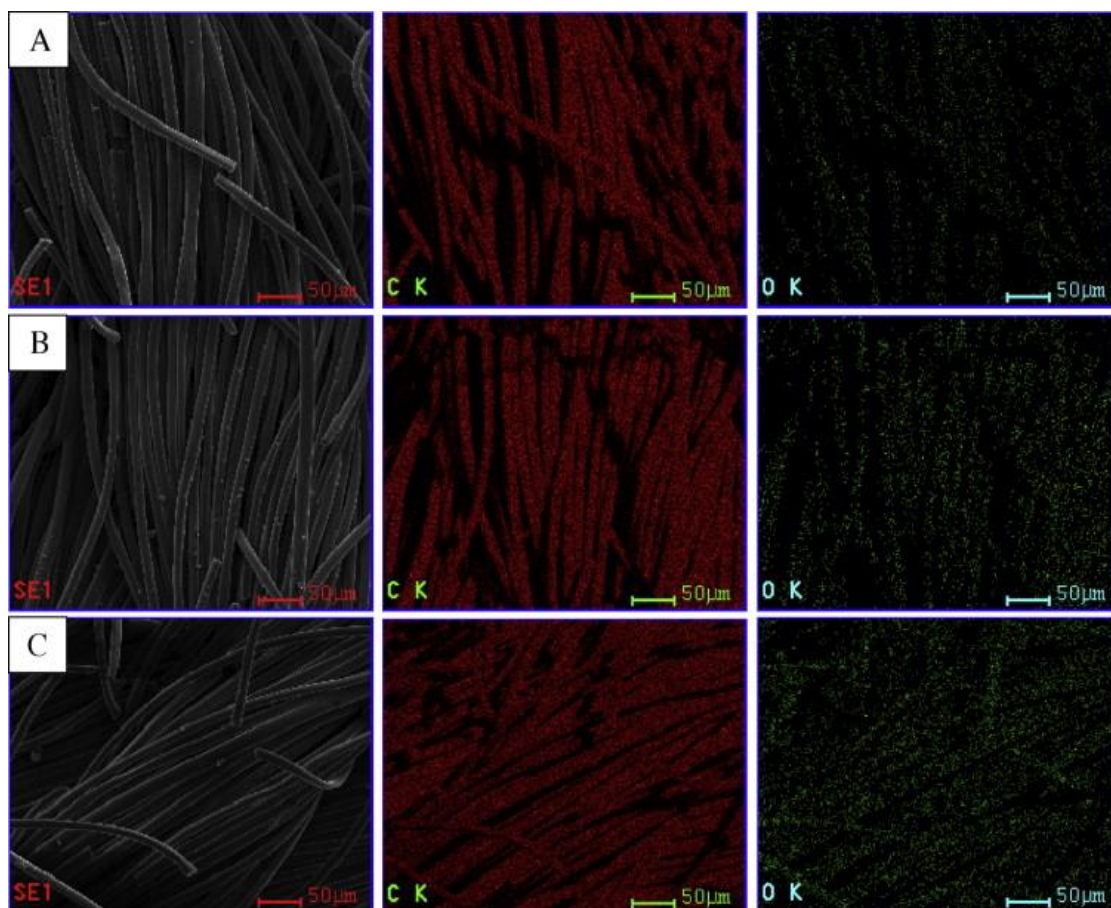
Figure 1.11. – SEM images with oxygen and carbon mapping by EDAX of ACC electrodes before and after long term operation with a flow-by cell. (A) A pristine ACC with initial 96.23 (wt%) of carbon and 3.77 (wt%) of oxygen. (B) The negatively polarized ACC electrode after long term experiment with 95.67 (wt%) of carbon and 4.33 (wt%) of oxygen. (C) The positively polarized ACC electrode after long term experiment with 91.84 (wt%) of carbon and 8.52 (wt%) of oxygen. The red and green dots represent the traces of carbon and oxygen respectively on the images [21].

1.5   Parasitic Faradic Reactions

The mechanism underlying ion storage in conventional CDI processes is the electrosorption of ions at highly porous electrodes. Physically, this ion storage process is capacitive by nature, in fact it consists in the accumulation of ionic charge at a liquid/solid interface, without transfer of charges across this interface. The latter kind of process is known as a faradic process. A real interface cannot be charged indefinitely, of course, and in the case of the a liquid/solid electrochemical interface, this means that along with charge accumulation at the interface via ion electrosorption, charge transfer may occur, through different reactions, depending on electrolyte, electrode material, and potential at the interface. Therefore, parasitic Faradic reactions may occur at both anode and cathode of a CDI cell. Under CDI operation, faradic reactions are likely to occur during the charging step, when a relatively high potential difference or current is applied to the cell.

The most frequently observed Faradic reactions are listed below:

Positive electrode:

- Carbon oxidation
- Water oxidation / Oxygen Evolution Reaction (OER)
- Chlorine evolution

Negative electrode:

- Oxygen Reduction Reactions (ORR)
- Carbon Reduction

Together with counter-ion repulsion, the abovementioned parasitic reactions are considered as a main source of efficiency loss in CDI system. Moreover, presence of charge-transfer reactions results in the worsening of electrode performance, decrease of energy efficiency and of electrode lifespan. In addition, these reactions cause the formation of chemical by-products and pH fluctuations of product water. Whilst other faradic reactions can improve desalination performance through pseudocapacitive or

intercalation effects, herein, the concern is with oxidation and reduction reactions not contributing to desalination [11].

Faradic reactions play a significant role in CDI operation, where energy consumed, and operational stability are significantly impacted by them. Reduction reactions take place at the negative electrode during charging, with oxygen reduction being the most common, while oxidation reactions occur at the positive electrode, including carbon oxidation, chloride oxidation, water oxidation, oxidation of inorganic ions and organic matters. Among the latter reactions, the most important is carbon oxidation, also for its deleterious effects such as pore structure impairment and mass loss, with subsequent decrease in carbon electrode longevity and deterioration of CDI performance.
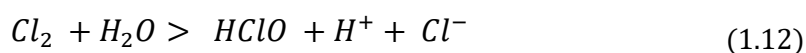
Carbon electrode oxidation has a negative impact on the performance and longevity of the CDI desalination process. It has a standard electrode potential of 0.21 V_{SHE}, which is within the usual CDI potential window. Therefore, during the desalination process, the carbon positive electrode undergoes oxidation. Carbon oxidation has different character depending on potential and electrolyte, and can be described by a series of reactions in an aqueous environment, see further on Reaction (**1.8**) to (**1.10**), that occurs at increasing potential. Carbon oxidation is a surface reaction, involving active sites at the surface, which may undergo oxidation by degree, starting with l the formation of surface carboxyl groups according to Reaction (**1.8**), with $E_0 = 0.21\ V_{SHE}$, then proceeding by further oxidation of the latter to the formation of carbonyl group ($C = O$) according to (**1.9**), to end up with the complete oxidation , at high potential and more generally under rather harsh conditions, to CO_2 with $E_0 = 0.9\ V_{SHE}$, according to (**1.10**) [11].

These oxidation processes may occur as direct oxidation when the positive electrode is polarized, leading to an increase in resistivity, a decrease in the surface area and pore volume, and induce changes to the pore structure decreasing the anodic ion electrosorption capacity. Strategies to evaluate the oxidation of CDI electrodes are based on monitoring the changes in the functional groups at the surface of electrodes using methods such as of X-ray photoelectron Spectroscopy, as the most effective analytical tool to characterize surface chemical modification, and possibly Fast Fourier Transform Infrared Spectroscopy, if large amount of material is available, Scanning Electron Microscopy, for general purpose morphology characterization, acid-base

titration, which also requires large amount of material, and Cyclic Voltammetry, as a versatile method to characterize electrochemical processes [11].

$$C + H_2O > C - OH + H^+ + e^- \quad (1.8)$$

$$C - OH > C = O + H^+ + e^- \quad (1.9)$$

$$C + 2H_2O > CO_2 - OH + 4H^+ + 4e^- \quad (1.10)$$
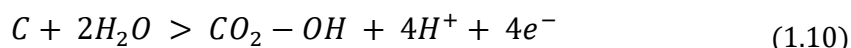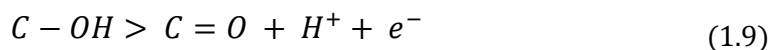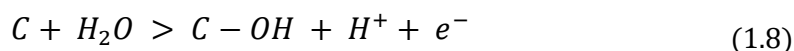
On the other hand, during the electrochemical treatment of brackish water, anodic oxidation of Cl^- following Reactions (1.11) - (1.13) and water (Reactions (1.14) and (1.15)) may occur provided a sufficiently positive potential is available. The mechanism involving Cl^- oxidation at the positive electrode starts with a direct oxidation of Cl^- yielding free chlorine (Cl_2). The free chlorine then rapidly hydrolyzes and disproportionate to form hypochlorous acid ($HClO$). $HClO$ then deprotonates forming ClO^{--} that can be further oxidized yielding chlorate (ClO_3^-). Further, provided a high enough positive potential is available (E^0= 1.47 V/SHE), the direct oxidation of Cl^- to ClO_3^- can occur at the positive electrode (Reaction (1.15)).

$$2Cl^- \rightarrow \rightarrow > Cl_2 + 2e^- \quad (1.11)$$

$$Cl_2 + H_2O > HClO + H^+ + Cl^- \quad (1.12)$$

$$HClO > H^+ + ClO^- \quad (1.13)$$

$$6HClO + 3H_2O > 3HClO_3^- + 4Cl^- + 1.5O_2 + 6e^- \quad (1.14)$$

$$Cl^- + 3H_2O > ClO_3^- + 6H^+ + 6e^- \quad (1.15)$$
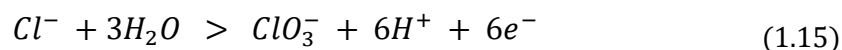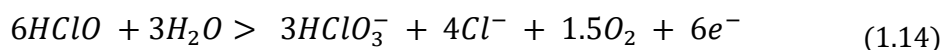
Oxygen evolution reaction (Equation (**1.16**)) has a relatively lower standard potential (1.23 V) than that of chloride oxidation (1.36 V), however, the reversible potential for the oxygen process depends on pH, while for the chlorine process it does not. On the

other hand, from the point of view of the kinetics, the oxidation of Cl⁻ has lower overpotential compared to the OER.

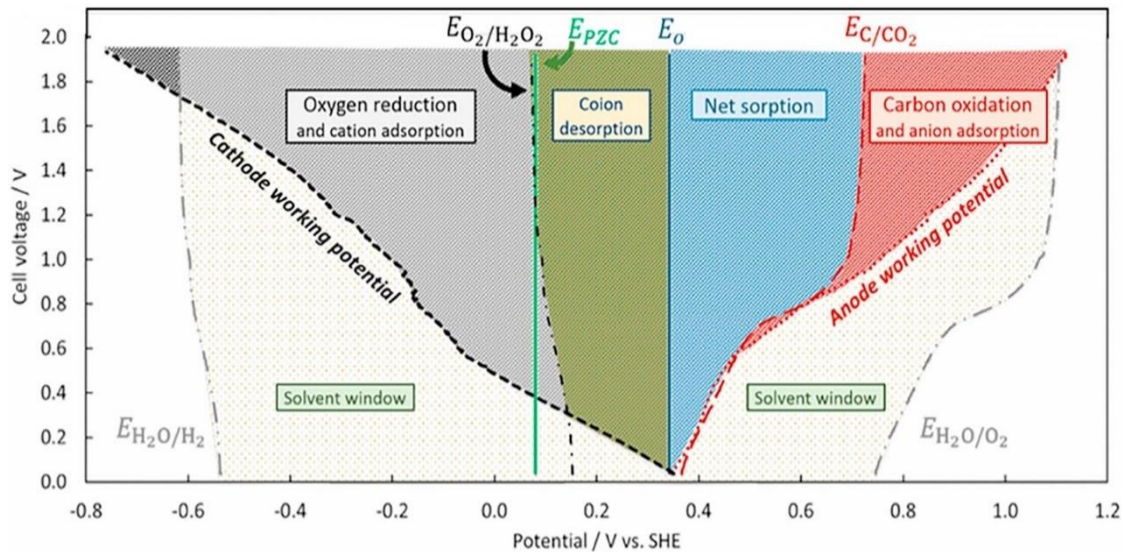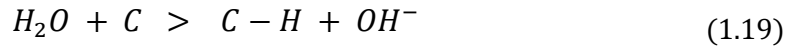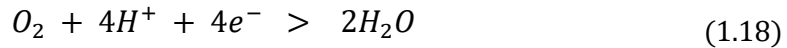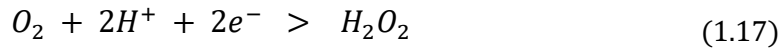$$2H_2O \quad > \quad O_2 + 4H^+ + 4e^-$$
(1.16)
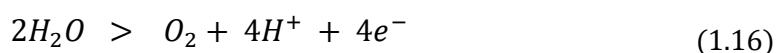
Overall, for the most common pH range of water streams, the oxygen process will be favored over the chlorine process. The latter may occur either in relative acidic condition (pH < 5) and/or at relatively high potential.

CDI process should be operated at cell voltage below 1.23 V to limit the extent of current leakage from water or slightly higher value, taking into account overpotential accompanying faradic processes. However, an asymmetric distribution of potential across the cell is likely to occur, because of the positive shift of the zero charge potential of the anode and possible pH fluctuations in the restrained space of a CDI cell. As a tentative semi-quantitative description of the likeliness of different faradic process in CDI, Figure 1.12 shows the potential distribution and the electrode processes that are possible at typical CDI working potential, below about 1.8 V [11].

Reduction reactions take place at the negative electrode during charging with oxygen reduction being the most common. There are two possible pathways for oxygen reduction: the $2e^-$ pathway (Reaction (1.17)), through formation of hydrogen peroxide or the $4e^-$ pathway (Reaction (1.18)). Reaction (1.17) is considered as the most probable. Oxygen reduction occurs when dissolved oxygen is present and can lead to an asymmetric potential distribution between the positive and negative electrodes, leading to an acceleration in the anodic carbon oxidation reactions in addition to pH fluctuations of effluent water. It is thermodynamically favored even at charging voltages as low as 0.6 V by the two-electrons pathway. On the other hand, though probably at significantly higher potential, carbon electrodes can experience cathodic reduction or hydrogenation resulting in the introduction of additional C-H groups (Reaction (1.19)). Actually, the evidence of carbon reduction at the cathode is yet to be conclusive [11]. The potential applied to CDI during salination/desalination operation, dictates the cathode and anode working potentials during operation, which then favor carbon oxidation and oxygen reduction reactions to occur in addition to sorption/desorption [22].

$$O_2 \ + \ 2H^+ \ + \ 2e^- \ > \ H_2O_2 \tag{1.17}$$

$$O_2 \ + \ 4H^+ \ + \ 4e^- \ > \ 2H_2O \tag{1.18}$$

$$H_2O \ + \ C \ > \ C - H \ + \ OH^- \tag{1.19}$$

Figure 1.12. Potential map of the possible electrode processes at typical CDI working potential [22].

1.6 Performance Enhancing Parameters

Performance of a CDI cell can be assessed by various parameters or figures of merit, such as specific energy consumption per liter of water produced, energy consumption per gram of salt adsorbed, grams of salt adsorbed at the electrodes, and electrode stability. In the experimental study of CDI systems, the assessment of performance is performed in order to optimize operating parameters. Among the most important parameters, there are the flow rate, the cell voltage, the specific electrode capacitance and the CDI cell volume. Each of these operating parameters may have different effects on the CDI cell performance. Therefore, optimizing the performance by studying the effects of these parameters, based on theory, simulations, or experimental work is of primary importance for the development of CDI technology.

The performance improvement of CDI systems occurs mainly by improving the electrode properties like capacitance, surface area, electrosorption, conductance and

25

pore size. Electrosorption capacity and kinetics of CDI electrodes can be tackled through various methods. These include the preparation of composite materials to improve the electrode capacitance, addition of carbon black to improve conductivity, addition of NaCl during electrodes preparation to improve the electrode permeability into electrodes increasing its macro-porosity, optimization of the electrode thickness for the desalination process, reducing the binder ratio in the electrode preparation to minimize blockage of pores. Furthermore, Ion- Exchange Membranes can improve the CDI cell performance in terms of salt removal, charge efficiency, and energy efficiency. Also, IEMs can significantly limit faradic reactions at the electrodes, hence tackling in particular the carbon electrode degradation problem and increasing the system stability [18].

It is common that operating parameters can have positive effects on some aspects of performance and negative for others. For example, increasing the cell potential positively impacts the SAC but negatively impacts energy consumption per liter of water/gram of salt adsorbed. This excess energy loss can be related to residual current consumed by faradic reactions with increased potential, leading to electrode deterioration and performance loss. Another important parameter is CDI cell volume, as increasing the cell volume negatively affects salt adsorption capacity and salt adsorption rate; also the energy consumption per gram of water increased with increasing the spacer volume. Finally, increasing the flowrate can decrease the energy consumption per liter of desalinated water, however water quality or the extent of desalination also decreases [18].

Overall, adjusting each of these parameters can prove beneficial to CDI performance. For optimum results, CDI cell volume can be reduced by applying pressure on the cell, reducing the free volume in the cell. Flowrate can be adjusted to a middle point balancing energy consumption and desalination performance. Nitrogen purge can be used to reduce dissolved oxygen in the feed solution, therefore minimizing carbon oxidation reactions to boost energy efficiency and operational longevity, though this measure is only practical in the context of laboratory work for research purposes. Electrodes can be socked in NaCl solution to optimize the pore structure for desalination [18].

1.7 Electrochemical Techniques

The use of various electrochemical techniques allows for the extraction of a wide range of data that can be used to understand the behavior of the CDI system. Each method utilizes either current or potential applied to the cell for a given period or with a given time dependence, and according to a measuring protocol, triggering different processes and reactions in the CDI system.

Open Circuit Potential

It is the potential when there is no current, also called equilibrium or rest potential. It is used to realize the shift of the anodic potential, for example, with reference to the cathodic one, giving, as an example, an indication for the shift of the anode potential with respect to the cathode potential, which is related to degradation.

Chronoamperometry

This technique consists in applying a constant potential to the cell and measures the current, which is related to adsorption processes at the electrode and parasitic reactions. The use of multi-step in CDI makes it possible to perform desalination experiments in the form of charge-discharge cycles, either at a single value or multiple voltage values. As an example, it can be used to charge the cell at 1000 mV for 10 minutes and then discharge at 0 mV for 10 minutes, for fixed number of cycles.

Cyclic Voltammetry

It is the basic test to learn about the electrochemical behavior of an electrode in a given electrolyte, where the current is recorded by sweeping the potential back and forth, usually applying first a positive scan up to a vertex potential, followed by potential reversal back to the initial potential applying a negative scan. The main parameter of the test, besides the range of potential, is the scan rate. By the visual analysis of a cyclic voltammogram it is possible usually to see oxidation and reduction (redox) peaks associated with faradic processes at the working electrode. Hence, the potential at which the electrode material is oxidized and reduced can be found [23]. Alternatively, in the

absence of such features, it is possible to recognize the the capacitive behavior of the electrode and evaluate its capacitance. The scan rate in mV/s and the potential window are determinant factors for the evaluation of the specific capacitance of the cell, following Equation (1.20)

$$C_s = \frac{\int_{E_0}^{E_1} I dE}{2mv(E_1 - E_0)} \tag{1.20}$$

where $\int_{E_0}^{E_1} I dE$ is area embedded in voltammogram performed over the potential window from E_0 to E_1 and m is the total electroactive mass of the electrode or electrodes, in case the measurement is performed on a cell.

Coulombic Efficiency is obtained from the CV data as per Equation (1.21), where charge density of the discharge cycle is divided by the charge density of the charge cycle, then converted to percentage values. Additionally, Specific Capacitance can also be obtained from the CV data, where the total cell capacitance is divided by two, then normalized by scan rate, applied potential, and electrode mass.

$$\Lambda_{CE} = \frac{Q_{ch}}{Q_{dis}} \tag{1.21}$$

where Λ_{CE} is the columbic efficiency, Q_{ch} and Q_{dis} are charges stored / released in corresponding charging/discharging cycles.

Electrochemical Impedance Spectroscopy

EIS is used to measure the impedance of electrodes or cells as a function of frequency, namely the frequency of the perturbation signal, usually a sinusoidal AC potential of small amplitude. The potential perturbation generates a sinusoidal current whose

amplitude and phase angle change with the frequency. The electrode or cell impedance is calculated as the ratio between potential and current and as a function of frequency [23]. Then, by varying the frequency of an applied sinusoidal cell voltage and measuring the change in the resulting current, an impedance response of the CDI cell is obtained. This response is a fingerprint of the processes occurring during the deionization process at different time constants; high frequencies correspond with fast processes and low frequencies correspond with slow processes. With EIS the dependence of resistance and capacitance as a function of frequency can be obtained, and thus the dependence of deionization rate and adsorption capacity on time [24].

Step Potential Electrochemical Spectroscopy

Step Potential Electrochemical Spectroscopy (SPECS) is an electrochemical technique designed for the separation of faradaic and non-faradic charge storage contributions in electrochemical capacitors. It allows for the deconvolution of the different components to the current response of the system, thus providing useful information for the study of the mechanism of charge storage, and the electrode behavior in general[25]. For CDI experiments, SPECS operate in a similar fashion to staircase linear sweep voltammetry making it possible to simulate the overall cell current as the sum of surface (i_s) and porous (i_p) double layer current, and residual current (i_r) as shown in Equation (1.22):

$$i_{tot} = i_s + i_p + i_{res}$$

(1.22)

Double layer current under potentiostatic conditions is described by an exponential decay function, according to Equation (1.23) and Equation (1.24):

$$i_s = \frac{\Delta E}{R_s} exp\left\{-\frac{t}{C_s R_s}\right\}$$

(1.23)

$$i_p = \frac{\Delta E}{R_p} exp\left\{-\frac{t}{C_p R_p}\right\}$$

(1.24)

where ΔE is the applied step potential, C and R are double layer capacitance and resistance formed in corresponding (surface and porous) parts of an electrode, and the

subscripts *s* and *p* stands for *surface* and *porous*. The model assumption is in fact that the capacitive response of the electrode / cell can be separated in two major contributions. One is related to the easily accessible surface of the electrode(s), also called "geometric" area, the other one to the porous surface area, then referred to as "porous" component.

The residual current is attributed to the presence of non-diffusion limited faradaic current or leakage current and assumed to be independent of potential, according to Equation (1.25):

$$i_{res} = const \qquad (1.25)$$

Chapter II

Materials and Methods

T he operational procedure to successful execute CDI experiments and obtain reliable results has been carefully examined and modified for optimum results. The main components of the procedure in-order are electrode fabrication, CDI system setup, electrochemical characterization, and data analysis. Given the interconnectedness of these steps and the complexity that arise from them, it was found that some operational factors affect the performance of the CDI system by impacting the values of SAC, ASAR, Charge Efficiency, and electrode stability. Therefore, the operational procedure used to determine the desalination performance and electrode behavior under various electrochemical tests was established for the best operability of the CDI system within the limits of this work.

2.1   Materials

Electroactive materials used in this work were either commercial or lab-made products. Commercial activated carbon YEC ® and conductive carbon Timcal ® are used as active materials and 60 wt. % water suspension of PTFE (Sigma-Aldrich ®) was used as a binder for electrode preparation. Ethanol (EtOH) and de-ionized water were used as solvents. Graphite plates (Alfa Aesar) with thickness 130 µm was used as a current collector. As a contact intermediate layer between electroactive material and current collector conductive glue E-dag ® was used. Diluted 10 mM NaCl solution was used as the electrolyte. Both AEM (150 µm) and CEM (160 µm) membranes were purchased from EURODIA.

2.2 Electrode Fabrication

The first step to fabricate CDI electrodes is making the appropriate electroactive paste of a composition set by weight percentages, as follows: 80% AC powder, 10% conductive carbon powder, and 10 wt. % PTFE. Both AC and CC powders are placed into a mortar and 10 ml of ethanol (EMSURE ACS) is added. The solution is mixed using a sonication probe for one minute. PTFE is added to the mortar in the form of dispersed solution and sonicated for another two minutes.

The mortar is heated uniformly using a hotplate, with a temperature range between 120 and 80°C for about 15 minutes, to intensify evaporation of the added ethanol. When the mixture turns towards a rubbery state, the mortar is taken away from the hotplate and the drying process is continued by motion using the pestle. It is then carefully gathered into a roughly spherical bullet and placed on a glass plate, before being flatten to a thickness of around 200 µm (measured by a Vernier caliper or a digital micrometre gauge) using a Teflon rolling pin. The paste is left to dry overnight at room temperature. Finally, 40×35 mm^2 rectangular cuts are taken from the paste and weighted. When two electrodes are within a mass proximity greater than 95%, they are used as a symmetric pair of carbon electrodes.

Graphite sheets are prepared for CDI use, by cutting it appropriately to the required dimension (59×37 mm^2), creating a fork shape at the top, and punching a hole (of 6 mm diameter) in the centre of the graphite sheet. Carbon glue is then applied on the main body of the sheet before placing the carbon electrodes on it. The whole structure is then pressed together in the oven at 80°C under the application of 5 kg mass for 10 minutes. Excess carbon pieces are cut in accordance with the graphite template and then weighted to determine the final electrode mass. CDI electrodes are then placed in ethanol/H_2O = 1/4 mixture, to remove air bubbles from the AC internal structure. Finally, CDI electrodes are pre-wetted by leaving them immersed in the 10 mM NaCl solution for at least 8 hours, as this allows sufficient time for the penetration of electrolyte into the pores of activated carbon, according to the experimental evidence.

## 2.3   Microstructural Characterization

Phase analysis of raw powders was performed by X-ray diffraction (XRD), with an instrument 1830 PW Philips X-ray generator equipped with PW 3020 Philips goniometer and a PW 3710 control unit. Cu Kα (λ = 1540 Å) was used. Thermo-gravimetric analysis (TGA) was performed in air with help of PerkinElmer Simultaneous Thermal Analyzer (STA 600). The heating rate was 10 ˚C min^{-1} until 900 ˚C. Microstructure of electroactive materials was studied by scanning electron microscope (SEM) using a Stereoscan 360 Cambridge SEM instrument.

2.4   CDI

The operational procedure for CDI revolves around four major areas: the system architecture, type of cell used, experimental procedure, and electrochemical characterization. System architecture revolves around the set-up of the pipeline and equipment used to run desalination experiments, while collecting data that can be used for analysis. Setting up the CDI cell plays a vital role in system response, stability, and performance due to the incorporation of anionic and cationic exchange membranes, proper cell spacing and sealing through proper tightening of the cell.

2.4.1   Pipeline

The setup used for the laboratory experiments is composed of the system components shown in Figure 2.1, consisting of a CDI cell, potentiostat, temperature probe, two pH probes and meters, and two electrical conductivity probes and meters. Also, a 10 L reservoir tank connected to a Masterflex peristaltic pump controller, a nitrogen gas pipe system, multiple control valves, by-pass pipe, and flexible pipelines connecting the whole apparatus.
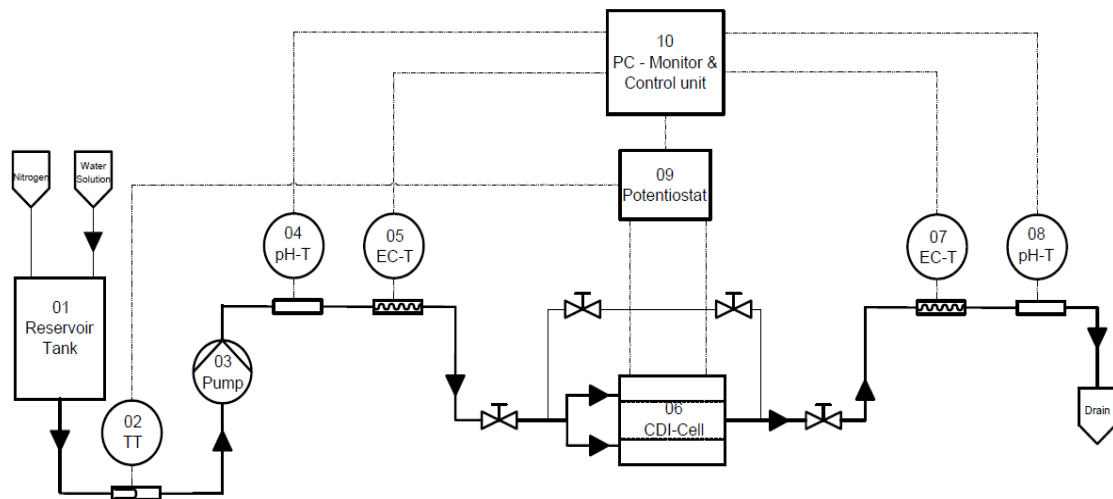
Figure 2.1. A Process Flow Diagram for the CDI operating system. TT: Temperature probe, pH-T: pH probe, EC-T: Electrical Conductivity probe. All probes measure changes in real time and transmit the signal to the monitor and control unit.

The reservoir tank has a capacity of 10 liters, that is filled and de-aerated by nitrogen purging prior to the start and during each experiment. The peristaltic pump controls the water flow out of the tank, i.e. the flowrate through the system. The pipelines connecting all the elements of the system, tubes, and fitting are in TYGON patented material (Saint-Gobain), with an internal diameter of 2.4 mm and 0.8 mm wall thickness. Desalination/regeneration cycles are performed using Constant Voltage mode with AMEL 2553 potentiostat/galvanostat. The potentiostat is connected to the cell with electrical wirings that are attached to the cell external electrical contacts using two alligator clips.

Five probes are used in the system, three at the inlet of the cell and two at the outlet, all operating in real time for the analysis of water flow. At the inlet, a temperature probe is connected to AMEL potentiostat-galvanostat model 2553, recording temperature with a resolution down to tone second interval. Next on the line, comes the pH probe connected to an AMEL pH meter model 338 followed by an electrical conductivity (EC) probe connected to AMEL conductivity meter model 160. At the outlet, the electrical conductivity probe is also connected to AMEL EC meter model 160, while the pH probe is connected to AMEL pH meter model 2335.

2.4.2   Cell

A flow-by single pass CDI cell was used for all the experiments. The cell is box-shaped, with a base of 10.8×7cm and a height of 4 cm. The top side of the cell carries holes for 16 hexagonal screws to achieve the desired extent of cell tightening by regulating the spacer channel height inside the cell, as well as three flow openings: two for the inlet flow and one for the outlet flow. The internal electrical contacts (small blocks of titanium) are gold plated, to prevent corrosion during use, and the sealing of the cell is achieved by using a silicon gasket fitting the dimensions of the cell.

The cell is composed of a few components that makes up the cell internal body structure. These components are placed in a certain order, maintaining the proper functioning of the cell as shown in Figure **2.2**. Starting from a bottom 1 cm thick shim, followed by the negative electrode facing up and then an anionic exchange membrane, if used. A plastic mesh (100 µm) is then placed on the top of the AEM to prevent short circuit between the upper and lower electrodes. Following up, a cationic exchange membrane (if used) is placed on the top of the mesh and then the positive electrode facing down. A 2 cm thick shim is then placed on the top of the positive electrode to hold the structure all together before the cell is closed. Finally, two channel-blocks are placed, one on each side of the cell, to keep the electrodes pressed against the gold-plated electrical contacts, then the cell is closed and properly sealed, leaving between 150 µm and 450 µm of free thickness between cell cover (a) and cell body (j) as shown in Figure **2.2**. The spacing is ensured by placing metal sheets (150 µm thick each) in between both parts described above. However, when both membranes are used in the cell, the minimum spacing is 450 µm whilst only 300 µm if one membrane is used. This is to accommodate for the thickness of membranes, ensuring a fixed internal cell free volume for all experiments and to control pressure inside the cell, facilitate solution flow through the cell.
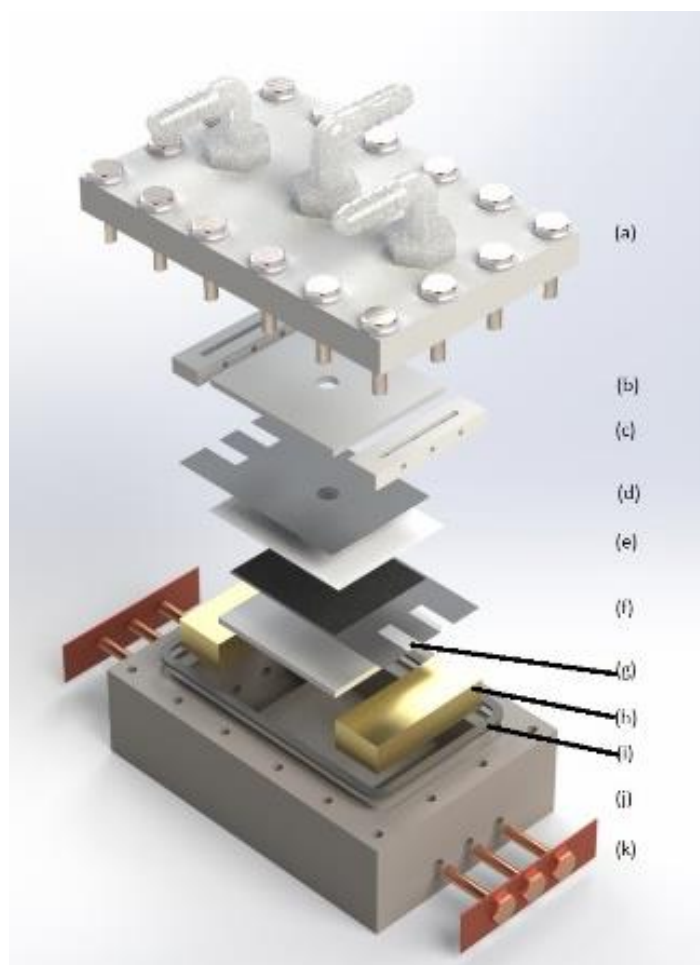
Figure 2.2. Internal components of CDI cell in order of arrangement. (a) cell cover, (b) 2 cm thick upper shim, (c) PTFE blocks, (d) positive electrode, (e) separator mesh, (f) negative electrode, (g) 1 cm thick lower shim, (h) gold-plated titanium blocks (internal electrical contacts), (i) silicon gasket, (j) Cell body, (k) External electrical contacts.

2.4.3   Experimental procedure

The main steps of preparing CDI system for experiments involve the preparation of 10 mM NaCl de-ionized water solution, proper calibration of pH probes, proper CDI cell setup, stabilization of the system, and finally running electrochemical checks. To begin with, a 10 L tank is filled with MilliQ water and then 5.844 g (± 1%) of NaCl is added to it, before being thoroughly mixed. Nitrogen flow is applied to the solution to purge dissolved oxygen for at least one hour before performing the first electrochemical test, while being left to purge for the entire experiment duration. Next comes the calibration of the pH meters by placing the probes in 2 buffer solutions with a pH of 4.0 and 7.0 in

an alternating manner while setting up the meter readings. This step was repeated multiple times to ensure the proper calibration of the pH meters.

CDI Cell is set up according to Figure **2.2** where a 1 cm thick shim is placed at the bottom of the cell, followed by the negative electrode facing up. In case of an AEM being used, it is applied on the top of the negative electrode. A separator mesh is then placed on the top of the AEM to prevent electrodes short circuit, followed by a CEM if it is used. Positive electrode is then placed facing down, while having all the middle holes align. A 2 cm thick shim is then placed on the top of the positive electrode, holding the overall structure together. A PTFE block is then placed on each side of the cell, to keep the electrodes pressed against the gold-plated current collector. The top of the cell is positioned, and all the 16 screws tightened. The volume inside the cell is a function of the extent of tightening, therefore a gap of around 150 µm between the cell top and cell body is maintained when no membranes are used, 300 µm when one membrane is used, and 450 when both membranes are used to allocate for membrane thickness.

The cell is then connected to the system via the tubes, the probes well positioned, and the pump started at a high flowrate (around 25 mL/min). The water flow initially is used to push out air bubbles from the system, with the help of temporarily increasing the pressure within the system by manipulating the manual valves. Additional bubbles can be removed by physically shaking the cell and the probes to push out any stuck air bubbles. Then the water flow is adjusted to the needed flowrate (normally 10 mL/min) before measuring the Open Circuit Potential (OCP) and running Multi-Step Amperometry (MSA) Charge-Discharge cycles, as shown in Figure 2.3, to check the proper functioning of the CDI system, electrodes performance and conditioning. The system is then kept stabilizing for around 30 minutes prior to the start of any electrochemical test.
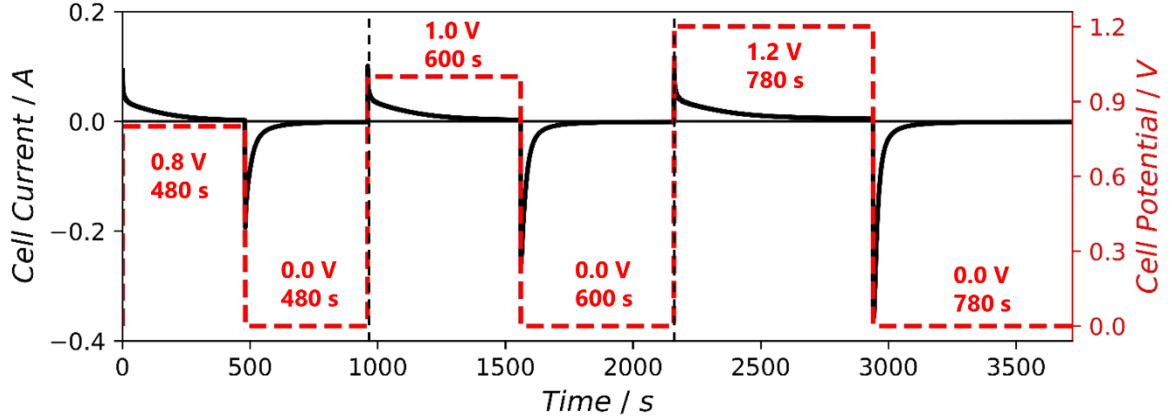
Figure 2.3 Charge-Discharge cycling procedure example: charging –first step of each cycle– at variable cell potential, as indicated, followed by regeneration under cell short-circuit (noted as 0 V). Step time changes depending on cell potential, as indicated.

Parameters used to describe the CDI cell, in terms of performance, are all calculated from the data extracted during operation, in particular conductivity and cell current. Apart from SAC (Equation (1.5)) and ASAR (Equation (1.6)), the following metrics are calculated as follow.

The concentration of NaCl is calculated using the Nernst-Einstein relationship, Equation (**2.1**), from the experimental determination of electrical conductivity, therefore is it used to derive the concentration profile as a function of time during CDI operations:

$$\sigma_m = \frac{F^2}{RT} \times (v_+ z_+^2 D_+ + \ v_- z_-^2 D_-) \tag{2.1}$$

where: σ_m is the molar conductivity, F is the faraday constant, R is the gas constant, T is the temperature, v_+ and v_- are the stoichiometric number of cations and anions respectively, z_+ and z_- valences of the ions, and D_+ and D_- are the diffusion coefficients of the ions.

Charge efficiency, Λ, is the ratio between the charge corresponding to the adsorbed salt (say, adsorption charge) over the total charge through the cell during each charging step. is the adsorption charge is derived from the integral of the concentration profile during charging step, multiplied by flow rate and by the Faraday's constant, F=96485

C mol^{-1}. This value can then be compared to the total charge given by the integral of the cell current during the same time interval. Final calculation as per equation (**2.2**).

$$\Lambda = \frac{VF \int [C_{out} - C_{in}]\, dt}{\int I dt}$$

(2.2)

2.4.4 Electrochemical Characterization

VApeak software is used to control the Amel potentiostat, to perform Multi-Step Amperometry (MSA) and Cyclic Voltammetry experiments, in addition to open circuit potential (OCP) readings. MSA is used primarily for performing desalination experiments, while OCP readings are recorded before and after individual runs to measure the extent of electrode degradation.

Other electrochemical techniques that utilize either DC or AC signals for a more in-depth analysis of the cell behavior were performed using Ametek (Solartron Analytical – ModuLab XM) potentiostat via the ModuLab XM ECS software control. Potentiostatic control, linear sweep voltammetry, cyclic voltammetry, Step Potential Electrochemical Spectroscopy, and Electrochemical Impedance Spectroscopy methods were used.

MSA Charge-Discharge is the main electrochemical test to run desalination experiments that can be elaborated to extract the key performance metrics in the CDI research field. Desalination experiments give a clear indication for the extent of degradation and operability of CDI. On the contrary, CV, SPECS, and EIS allow for in-depth analysis of the CDI electrodes and the system. In this work, desalination experiments were performed to analyse the generic effect of flowrate on the salt adsorption capacity by running 3 charge-discharge cycles at 1000 mV – 0 mV using the same electrodes, at each flowrate. This was done to fix all variables of the system such as: electrode variation, solution variation, cell tightening, room temperature, and probes calibration.

Degradation experiments are executed on fresh electrodes, using charge-discharge at 1000 mV – 0 mV cycling for at least 14 hours of operation. These experiments start directly after the system preparation, to measure the extent of prolonged cycling with minimal interfering factors. A similar approach is used for CV and SPECS experiments, where a single electrode is used for the whole duration of each experiment. CV

experiments are performed at 1mV s^{-1}, performing three cycles at each potential interval. The range starts at 100 mV (potential sweep range from 0 to 0.1 V), all the way to 1000 mV (potential sweep range from 0 to 1 V) at 100 mV intervals, therefore covering ten potential windows.

Following CV, EIS is performed at the same potential window as CV, starting at 100 kHz, ending at 1 mHz, with an amplitude of 20 mV. Following that, SPECS is performed as a series of incremental increase in potential from 0 mV to 1000 mV, in 25 mV increments, increased every 300 seconds. When 1000 mV is reached, the process is reversed down to 0 mV in the same 25 mV increments decrease every 300 seconds. Therefore, there are a total of 81 steps, 40 from 0 to 975 mV then 1000 mV followed by 40 steps down to 0 mV. For all these experiments, pH and electrical conductivity are measured to extract key metrics and useful data. Finally, OCP is measured before and after each run to determine the shift in anodic potential with respect to the cathodic one, indicating the extent of carbon oxidation by the asymmetry induced.

For all experiments, cell current and voltage are measured by the potentiostat to determine charge efficiency of the CDI cell. Additionally, electrical conductivity and pH of the effluent solution is measured with a reading resolution of 1 second interval. Electrical conductivity of the influent solution is also measured and used to determine the difference in electrical conductivity (outlet – inlet). On the other hand, pH readings give an indication for possible faradic reactions that occur under each cell condition, as a function of the electrochemical test applied to the CDI cell. For CV, SPECS, and EIS, additional cell data such as charge density, current density, and cell impedance are obtained from the potentiostat to determine coulombic efficiency, specific capacitance, residual current, and time constant of the cell electrodes allowing for in-depth analysis of the cell behaviour under various cell configurations and operating conditions.

Chapter III

Results and Discussion

Electrochemical performance of CDI depends on a wide range of variables including the active electrode material, cell configuration, salt solution, and operating parameters. Herein, we examined the main methods for optimizing the electrochemical performance, while attaining an in-depth analysis of the effect of faradic reactions on the CDI system. We observed that there are three cell potential regions where the system behaves differently: the potential range from 100 mV to 500 mV can be considered as a "safe region", while the potential range from 600 mV to 800 mV is considered as an "intermediate region", where the onset of pH fluctuations occur in parallel with higher residual current indicating the onset of parasitic reactions. Finally, the extent of degradation and pH fluctuations increase remarkably for cell potential higher than 800 mV, negatively affecting the system stability and electrodes prolonged performance.

3.1   Optimization of CDI Operating Parameters

Capacitive deionization technology remains a relatively new technology that is yet to be fully understood. For that, every CDI architecture and operating parameter has a significant impact on the cell electrochemical behavior and performance. Herein, an attempt to establish an optimum cell preparation procedure covers aspects such as choice of electrode material composition, electrode preparation, CDI cell assembly

procedure and tightening, effect of flowrate on desalination performance, and long-term pH and performance stability. Electrode preparation and cell tightening are a preliminary requirement to ensure a reasonable control and reliable operating functionality of the system, prior to the experimental study of the effects of operating parameters on performance and operational stability.

3.1.1 Microstructural Characterization

Active material in CDI electrodes is majorly responsible for the performance and electrochemical behavior of the cell. The choice of activated carbon as the active material is based on the expectation of a higher specific capacitance value due to higher specific surface area on the size distribution and particles size, thus promising high salt adsorption capacity during salination-desalination experiments. In Figure 3.1 (a) and (b) we observe AC YEC SEM images, which show the particulate nature of the pristine powder, with average particle size that can be estimated about 13 μm. As explained previously, the electrode paste incorporates conductive carbon and polytetrafluoroethylene. The former is to improve the conductivity of the mixture compensating for AC YEC conductance, while the latter binds well AC and CC to form a uniform activated carbon paste and helps adhesion to the current collector. Figure 3.1 (c) and (d) show the appearance of the electrode paste, with the characteristic granular morphology which suggest the macroporous structure of the layer. Conductive carbon particles can be easily discriminated from activated carbon particles as finer particles, while PTFE can be seen as long bands on the surface of AC particles.
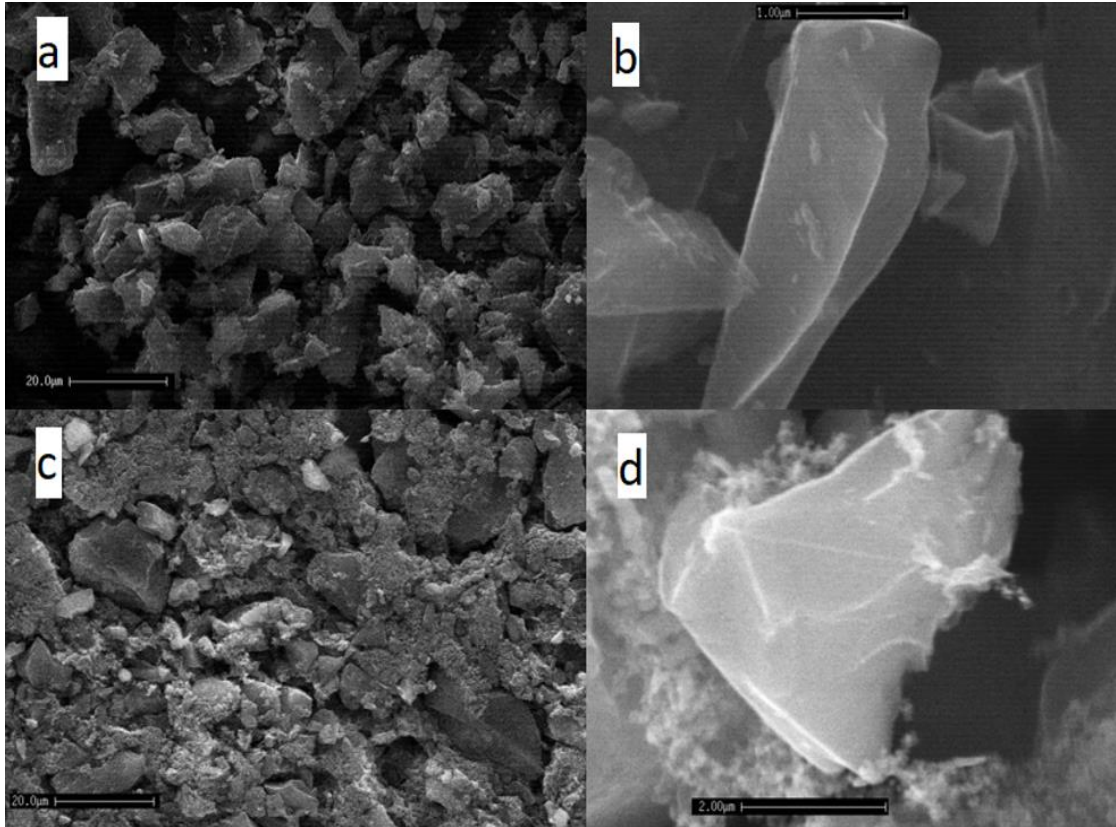
Figure 3.1. SEM image covering 11 mm material width of: AC YEC a) at 1000X magnification, and Sb) 24000X magnification, the mixture AC-YEC: CC: PTFE (80:10:10 ratio respectively by weight) c) at 1000X magnification, and d) 15000X magnification.

CDI electrodes are primarily responsible for the cell electrochemical behaviour and desalination performance, therefore the process of electrode fabrication and preparation, including conditioning before and after cell assembly, needs to be very well tuned for optimal electrochemical performance. As activated carbon is the base material for the CDI electrodes, where the pores are mainly responsible for the adsorption of charged ions in the influent solution, the extent of pore wetting has a considerable effect on the initial desalination performance. This is due to the presence of a diverse pore size structure: macro (> 50 nm), meso (2-50 nm), and micro (< 2nm) pores, all present in its highly branched internal structure with an advantageous high specific surface area, of up to 2500 m^2g^{-1}.

3.1.2 Preconditioning of the electrodes

Due to the nature of AC electrodes, it takes considerable time for the electrode to be completely wetted or, in other words, for the pores to be filled by the electrolyte, which can be reflected in desalination experiments. It is realized that pre-soaking electrodes

in the ionic solution (10 mM NaCl) for at least 8 hours prior to CDI operation significantly boosts adsorption-desorption performance. Ideally, electrodes are kept overnight with the beaker top sealed to reduce the rate of air dissolution in water and thus the amount of dissolved oxygen in the NaCl solution. Figure 3.2 shows an example of the influence of soaking time, or more precisely in this specific case of both soaking time and cycling, on the adsorption capacity of the cell. A clear change in behaviour, and in fact enhanced adsorption, is observed after 10 hours of operation. We took this as an indication that soaking time is a relevant parameter for optimal CDI performance. For that experiment, electrodes were directly put in the cell and used for CDI right after fabrication. The flowrate is 10 mL/min, the cell potential is at 800 mV for 8 minutes, at 1000 mV for 10 minutes, and at 1200 mV for 13 minutes, respectively per each cycle, while discharge occurs at short circuit (0.0 V) within the same time duration of the charging cycle.
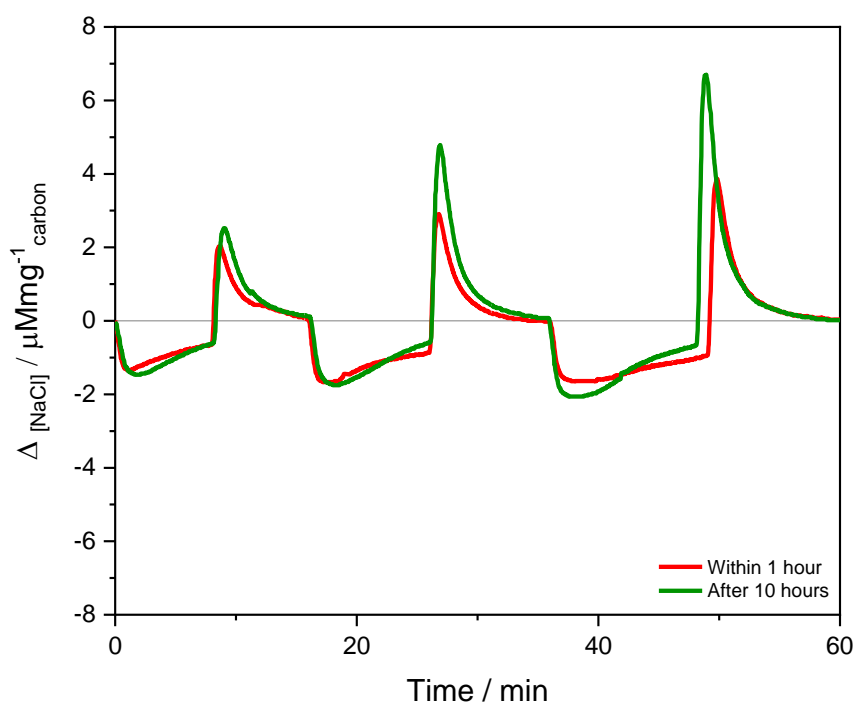
Figure 3.2. Experimental results for unsoaked AC electrodes, showing the change of electrolyte concentration (10 mM NaCl) within several charge-discharge cycles at increasing charging potential.

3.1.3 Tightening and Flow Rate

A major step in CDI cell assembly is final tightening of the cell using the 16 screws that attach the cell cover with the cell body as shown in Figure **2.2** shown in Chapter II. The main purpose of this procedure is to bring closer all components inside the cell, whilst reducing the free volume within the cell to allow for a close proximity between the positively charged electrode and the negatively charged one. The proximity makes more efficient the adsorption-desorption of ions at the surface of the electrodes , reducing overall resistance to ionic transport. As such, a tighter cell should correlate with higher values of salt adsorption capacity and vice versa. To elaborate on the importance of tightening for CDI performance (based on the SAC metric),
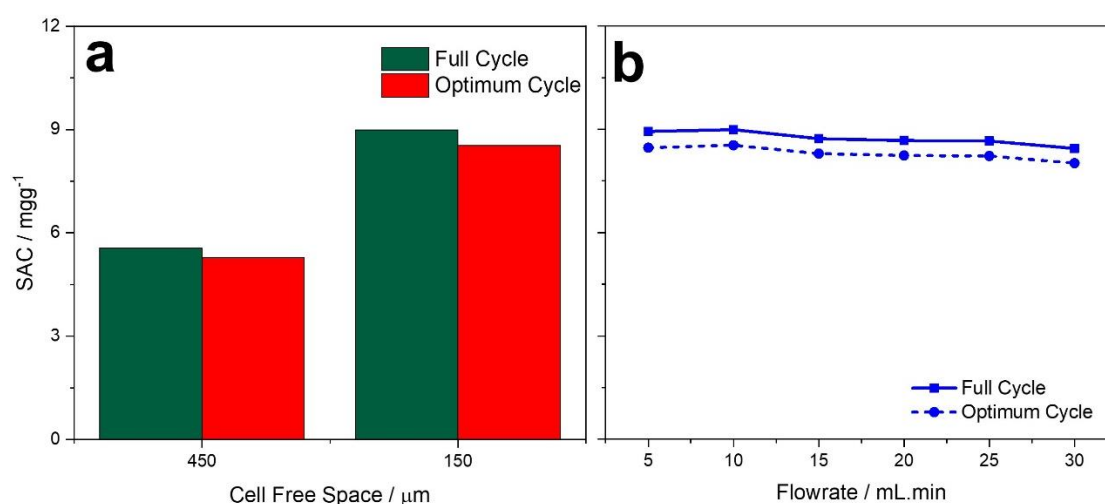
Figure 3.3 (a) shows a comparison between well tightened and loose CDI cells, where the cell is charged at 1000 mV while discharged at 0.0 V. This result indicates the inverse proportionality between cell free volume and SAC values. When cell tightening brought down to 150 µm the gap between the cell top and cell body, by strong screwing, SAC values were higher by over 30% with respect to tightening to a gap of 450 µm. This behaviour persists across flowrates from 10 to 30 mLmin^{-1}, notwithstanding the fact that SAC is evaluated at 95% salt adsorption or over the complete cycle, at 100% salt adsorption.
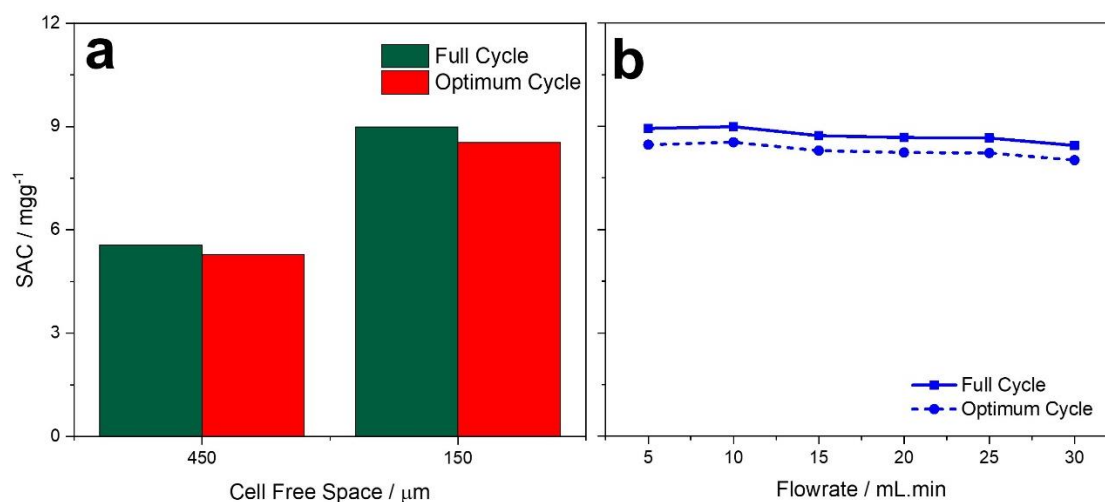
Figure 3.3 a) A comparison of CDI performance in terms of SAC, at 10 mLmin⁻¹, between a well tightened cell (150 µm gap between cell top and cell body) and relatively loose cell (450 µm). b) Effect of CDI system flowrate on desalination performance based on SAC metric.

The flowrate through CDI system contributes to the internal pressure of the CDI cell. However, once the cell is tightened thoroughly to 150 µm, the cell flowrate between 5 mL.min⁻¹ to 30 mL.min⁻¹, does not seem to have a significant impact on the cell desalination performance as shown in Figure 3.3 (b). This observation indicates that once the electrodes inside the cell are within a set limit of proximity, the flow rate, within the range tested in this work, does not affect the performance of the cell, namely SAC and ASAR values. Notwithstanding other and more subtle effects, this result suggest that minimizing the cell free volume is an essential requirement towards optimization of desalination behavior.

3.1.4 Degradation Phenomenon

The use of capacitive deionisation for purposes of brackish water desalination raises concerns on prolonged electrode stability and performance in presence of faradic reactions. The main electrode material, activated carbon, has a relatively low stability under conditions of anodic polarization, which worsens as the potential increases and in acidic environment, as well as with increasing temperature. Anodic polarization triggers a chain of electrochemical reactions that compromise long-term stability and performance of AC based electrodes. As already discussed previously, faradic reactions may occur both at the positive electrode (carbon oxidation, water oxidation / oxygen

evolution reaction (OER), chlorine evolution) and at the negative electrode (oxygen reduction reactions (ORR), carbon reduction). Together with the phenomenon of co-ion repulsion, the abovementioned parasitic reactions are considered as a main source of efficiency loss in CDI system.

This efficiency loss can be observed in a degradation experiment, shown in Figure 4 (a), carried out over a flowrate of 5 mL.min^{-1} and time range of 14 hours, charging at 1 V for 10 minutes while discharging at 0V for the same duration. Visually, it is possible to observe the decline in $\Delta_{[NaCl]}$ with time, indicating performance degradation. Additionally, by calculating SAC for a number of cycles, the extent of degradation can be seen in Figure 4 (b), with an extrapolation of the declining slope of SAC suggesting that SAC could reach very low value within several hundred cycles of operation, in other words within few days.
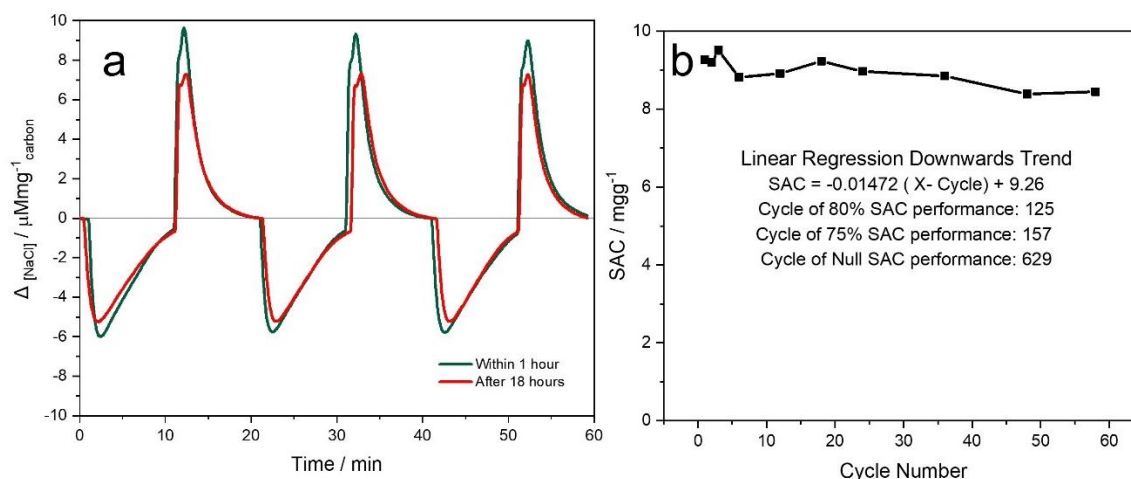
Figure 4. a) Comparison between desalination cycles within the 1st hour and 18th hour to indicate possible degradation. B) Determination of the linear degradation trend.

Moreover, the presence of charge-transfer reactions results in the decrease in electrode performance, energy efficiency, and electrode lifespan. These reactions cause the formation of chemical by-products and pH fluctuations of the fresh water produced, that may be a threat to operational stability as well. Figure 5 shows an example of pH fluctuations, where the cell was charged for 10 minutes at potentials of 0.7 V, 0.8 V, 0.9 V, and 1.0 V consecutively, while discharged at 0 V for the same duration, for every cycle. The number of cycles has a significant impact on pH profiles. By the way, this observation highlights the importance of the initial cycling of the cell before obtaining a reasonable stable behaviour.

47

Additionally, pH fluctuations seem to be a function of the potential applied to the cell, confirming the possibility that the incidence of faradic reactions becomes more important at higher potentials.

With cycling, pH profile may change substantially, because of the concomitant degradation of the positive electrode, as shown in Figure 5. Upon cycling, surface oxidation (formation of oxygenated groups at the surface) has the effect of depressing the rate of oxidation, as revealed by pH changes, likely because of saturation of most reactive surface sites. Higher cell potential, as 1.0 V, can still sustain high rate of degradation, in fact.

Thus, pH fluctuations coupled with performance degradation are clear indications that carbon oxidation reactions occur with their deleterious effects such as pore structure impairment and mass loss, with subsequent decrease in carbon electrode longevity and deterioration of CDI performance.
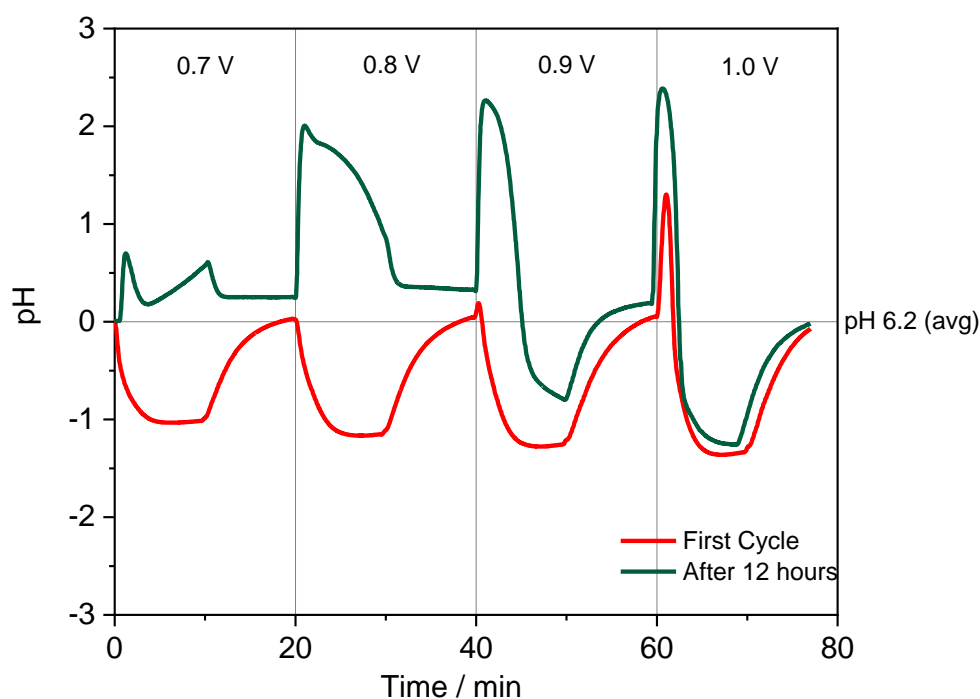
Figure 5. Effect of potential and prolonged operation on pH profile.

3.2 Electrochemical Analysis

Electrochemical analysis of the CDI system was performed to shed light on the effect of potential on the system response and in the attempt to clarify the importance of faradic processes with regards to energy efficiency. This is stemming from the

48

conception that the main source of carbon electrodes degradation and system instability is the presence of faradic reactions. Those reactions are directly correlated with the applied potential, as the higher the potential after the minimum threshold, the more likely a reaction would occur and to a greater extent. Thus, Cyclic Voltammetry and Step Potential Electrochemical Spectroscopy techniques were used to study the behaviour of the cell over a broad range of potential and different charge/discharge scan rates.

3.2.1 Cyclic Voltammetry

CV are performed to study the electrochemical behavior of the activated-carbon electrodes by sweeping the potential back and forth, with a positive scan of the potential up to a vertex value, followed by the reversal of scan direction towards the initial value. Therefore, cyclic voltammetry is performed over a specific range of potential, first by a positive scan, then by a negative scan, while recording the current. CV experiments were performed at the scan rate of $1 \ \mathrm{mVs^{-1}}$, in three successive cycles for each potential window. The range of potential starts at 100 mV, all the way to 1000 mV, by increasing it at 100 mV intervals, therefore covering ten potential windows. The current vs potential profile of a CV scan gives an indication of the onset potential of faradic reactions, and of their relative importance by the value of the current, as shown in Figure 6 below. It is clear from the high potential tail in the CV curve of the CDI cell, that the cell in the absence of membranes, shows the earliest onset of charge transfer and the highest charge transfer rate. The AEM-CDI and CEM-CDI cells show an overall similar behavior; however, it is apparent that the high potential tail is relatively more important with the AEM-CDI cell. In addition, the area enclosed by the CV is slightly larger compared to the CEM-CDI cell, meaning that the AEM-CDI promises better performance in terms of salt adsorption capacity, as we reported in a previous section. The shape of the CV for the mCDI cell is peculiar because of the strong reduction of the current at low polarizing potential, while as the latter increases there is a relative increase of the current with respect to the other cells. Supposedly, these peculiarities of the mCDI cell are the effects of ionic selectivity and inhibition of charge transfer by the membranes.
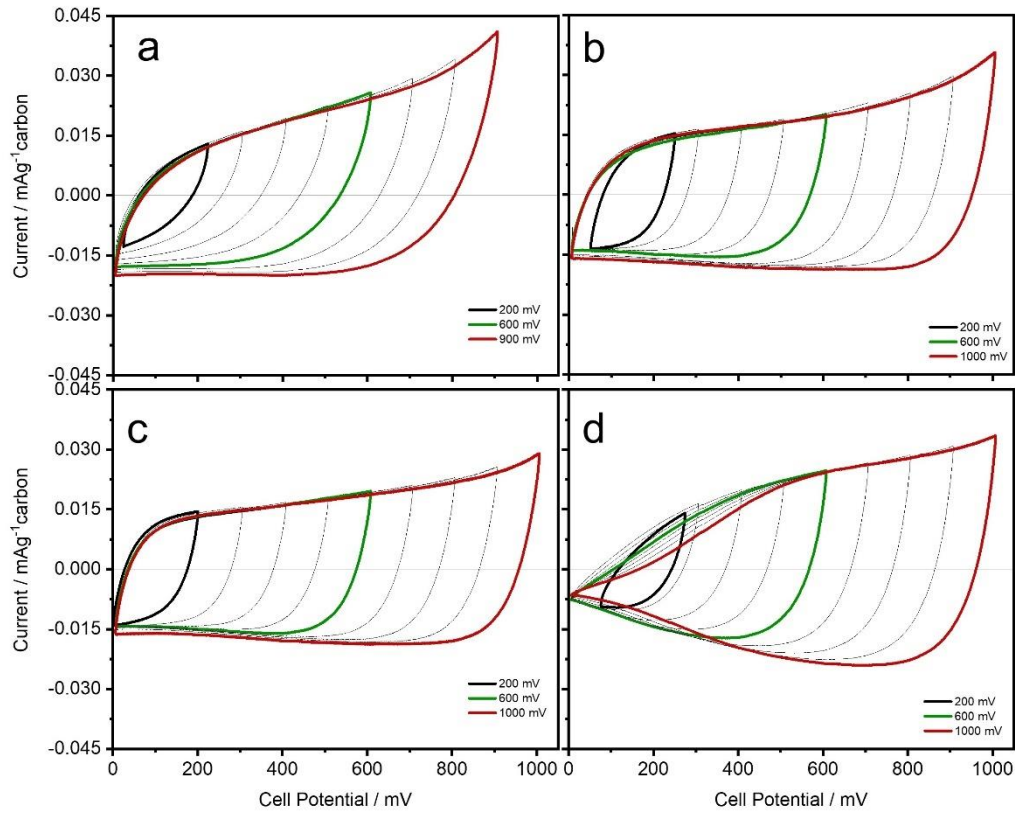
Figure 6 CV profiles of a) CDI cell, b) AEM-CDI, c) CEM-CDI, and d) MCDI.

Variations in pH profile during CV experiments give a clear indication for the possible reactions responsible for carbon electrodes degradation by correlating the pH movements to its corresponding reactions. Increasing acidity implies the possible cause being carbon oxidation and oxygen evolution reactions, since the concentration of H^+ is linked to faradic reactions at the positive electrode such as:

for carbon oxidation:

$$C + H_2O > C - OH + H^+ + e^- \tag{3.1}$$

$$C - OH > C = O + H^+ + e^- \tag{3.2}$$
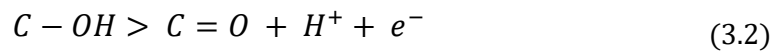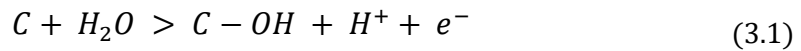
For oxygen evolution:

$$2H_2O > O_2 + 4H^+ + 4e^- \tag{3.3}$$
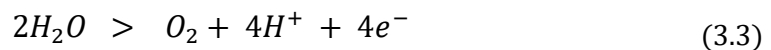
As oxygen evolution reaction occurs at higher potential values than that of carbon oxidation reaction, a more aggressive extent of acidification at higher potentials could be expected. However, it is difficult if not impossible the occurrence of this reaction at

50

the anode with a cell potential window of 1.0 V. Then, this reaction will not be considered in the following discussion.

Figure 7 shows the degree of acidification during cyclic voltammetry experiments of CDI, AEM-CDI, CEM-CDI, and MCDI. The extent of acidification or H^+ concentration increase is more favorable when no membranes were used (CDI) due to the lack of inhibition of faradic reactions. On the contrary, the use of AEM had the least acidification from potentials of 100 mV up to 700 mV for all configurations. However, at higher potentials (900 and 1000 mV), the use of anionic exchange membrane did not have a considerable effect on inhibiting carbon oxidation, on the contrary it led to a relatively strong acidification, like in the CDI cell.
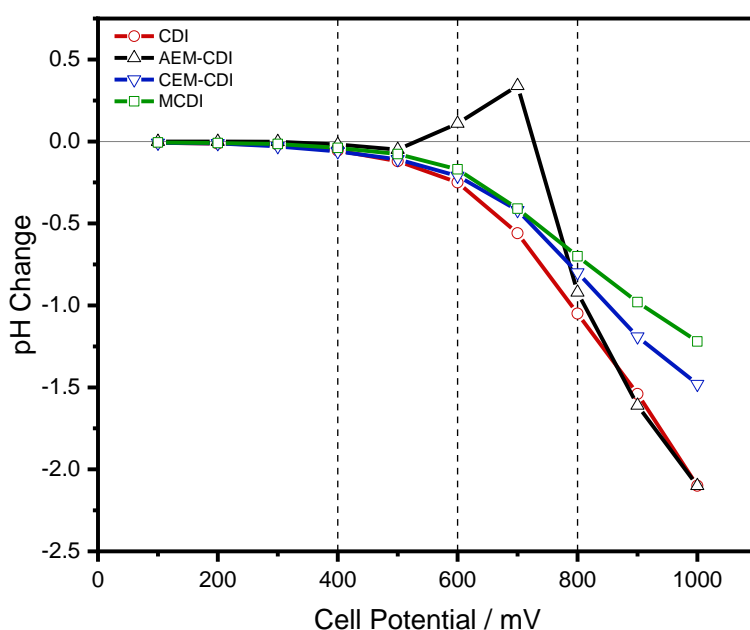
Figure 7. Degree of Acidification during cyclic voltammetry experiments.

The use of AEM does not inhibit however oxygen reduction (reactions (**1.17**) and **Error! Reference source not found.**) and carbon reaction **Error! Reference source not found.** reactions, which occur at the negatively charged electrodes. Nevertheless, H^+ ions are required for oxygen reduction reactions at the cathode; therefore, the reaction would accelerate in acidic environments.

$$O_2 + 2H^+ + 2e^- \rightarrow H_2O_2 \qquad (3.4)$$

$$O_2 + 4H^+ + 4e^- \rightarrow 2H_2O \tag{3.5}$$

$$H_2O + C \rightarrow C - H + OH^- \tag{3.6}$$
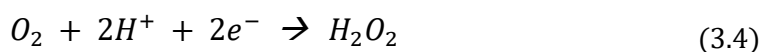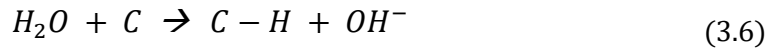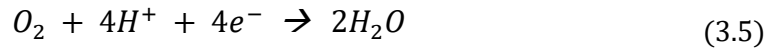
This can explain the initial alkalinization during AEM-CDI experiment, as oxygen reduction possible occurred at the negative electrode before oxygen evolution takes place. Alternatively, the lack of alkalinization observed when operating with CEM-CDI and MCDI is a result of the suppression of faradic reactions occurring at the cathode.

Figure 8 (a) shows columbic efficiency data derived from CV curves. There are obvious differences between the cells with both or a single membranes and the membrane-less cell CDI. This confirms the strong effect that membranes have on faradaic reactions, in general. On the other end, the trend is decreasing for all configuration, and in a similar way, which suggest that, as far as faradic losses are concerned, there are similarities between the different configurations. This observation suggest also that carbon oxidation is the most important process in this regard, since it may occur notwithstanding the presence of the AEM, provided the potential is high enough. In fact, the mCDI configuration shows the highest values over the entire range of potential, thanks to the effective suppression of the oxygen reduction reaction, on the one hand, and a relative shift of the onset potential of carbon oxidation, at least as a possible explanation. Actually, a different interpretation is that in the presence of CEM, there is in any case a relative more symmetric distribution of potential, and therefore the actual potential at the anode is lower than, for example, in the CDI cell or also in the AEM-CDI cell. This seems to be confirmed by the fact that the AEM-CDI cell shows relatively lower value of coulombic efficiency over the all range of potential compared to the CEM-CDI. As a final remark, it should be emphasized that cyclic voltammetry alone is not sufficient to draw strong conclusion about the relative importance of faradic processes at changing cell configuration. Therefore, the above discussion should be regarded as a provisional interpretation.
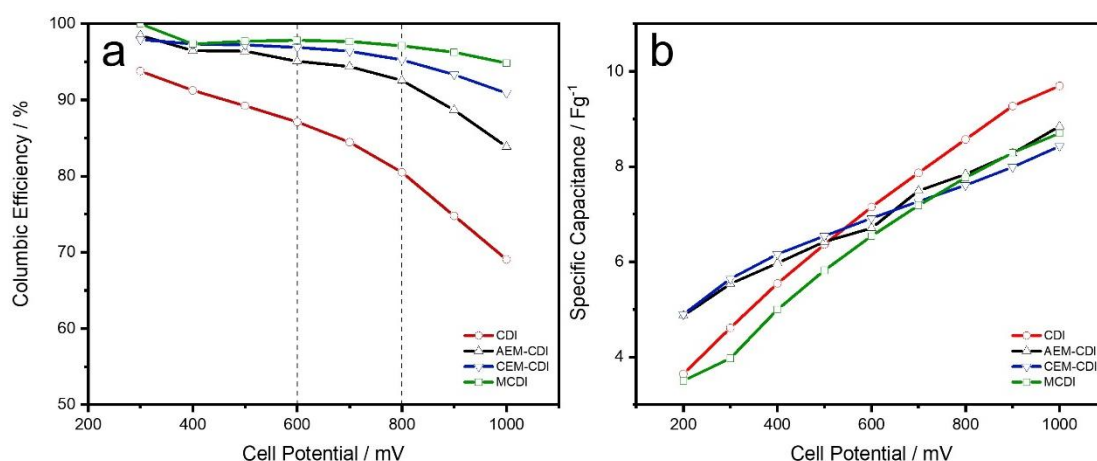
Figure 8 a) Columbic efficiency as a function of cell potential. **b)** Specific Capacitance as a function of cell potential.

3.2.2 Step Potential Electrochemical Spectroscopy

Step Potential Electrochemical Spectroscopy (SPECS) is an electrochemical technique designed for the separation of faradaic and non-faradic charge storage contributions in electrochemical capacitors. It allows for the deconvolution of the current response of the system into its components that corresponds to the diffusion and activated controlled mechanisms of charge storage, therefore determining the mechanism of charge storage, and electrochemical capacitor performance. SPECS is performed as a series of incremental increase in potential from 0 mV to 1000 mV and backwards, in 25 mV increments applied every 300 seconds. Therefore, faradic reactions can occur over a broader timeframe making it possible to realise the effect of potential on pH and therefore the underlying parasitic reactions responsible for such variations.

In Figure 3.9, we observe the pH variations across potentials during both charging and discharge cycle. The smaller potential increments allow for reactions with relatively slow rate to occur, thus increasing the possibility of higher pH variations. Similarly to CV results; CDI, AEM-CDI, and MCDI show similar trends of pH variations as a

function of potential. For CDI and MCDI, faradic reactions responsible for acidification (carbon oxidation and oxygen evolution) dominate by increasing the concentration of H^+ ions. Additionally, the same trend for AEM-CDI is observed, where at lower potentials (less than 800 mV), alkalinisation is primarily observed followed by aggressive acidification at higher potentials. However, CEM-CDI shows initial alkalinisation followed by acidification, contradicting CV result at lower potentials. A possible explanation is that the extended timeframe within which potential was applied to the cell, allowing the diffusion of dissolved oxygen through the membranes, triggering oxygen and carbon reduction reactions to occur. Whilst at higher potentials, the extent of carbon oxidation significantly increased, pulling down the pH to acidic values. MCDI shows the least overall pH fluctuation in comparison to other configuration, due to the suppression of both positive and negative electrode faradic reactions. Lower pH fluctuation implies higher operational stability, lower degradation, and therefore more reliable desalination performance.
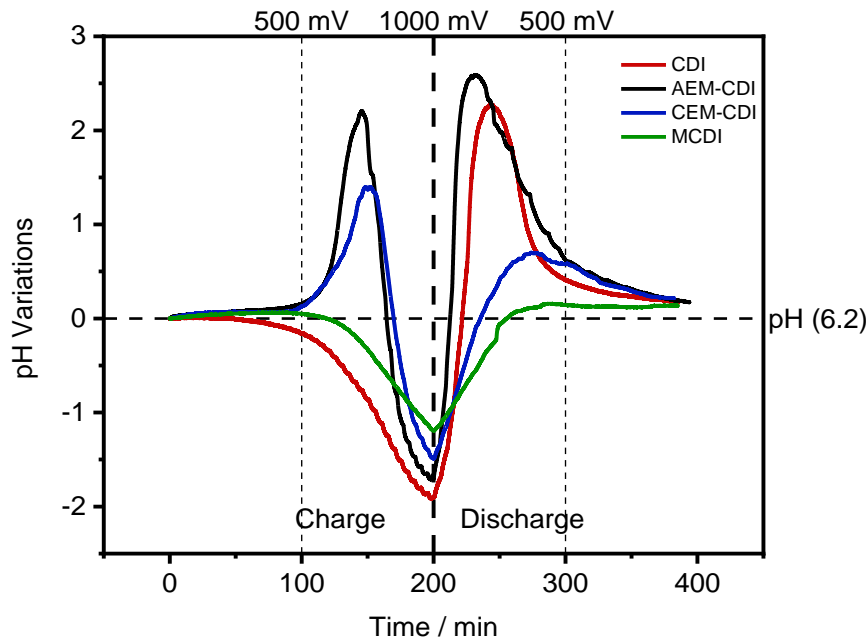
Figure 3.9. pH variations with time during SPECS analysis.

Residual current is a measure of current consumed by non-capacitive interactions, thus relating to parasitic reactions. In Figure 9 (a), the use of either AEM or CEM shows a

54

significant reduction of residual current due to the suppression of parasitic reactions, with MCDI having the lowest residual current at all potentials. Additionally, pH fluctuations seem to be correlated with residual current values. This can be observed from the Figure 3.9, where CDI had the highest degree of acidification, followed by significant pH fluctuations of AEM-CDI, lower degree of pH variations of CEM-CDI, and the lowest degree of acidification of MCDI. This directly correlates with the pattern observed in Figure 9 (a), where CDI had the highest residual current values, followed by AEM-CDI, CEM-CDI, and MCDI orderly. Nevertheless, double layer capacitance of the porous layer, shown in Figure 9 (b), has similar values for all CDI configuration particularly after 300 mV. This suggests that electrochemical performance of CDI is not significantly impacted by using ionic exchange membranes, leading to possibly similar desalination performance. Additionally, operating between 600 mV and 800 mV would be an optimum balance between electrochemical performance and operational stability by means of avoiding extensive faradic reactions.
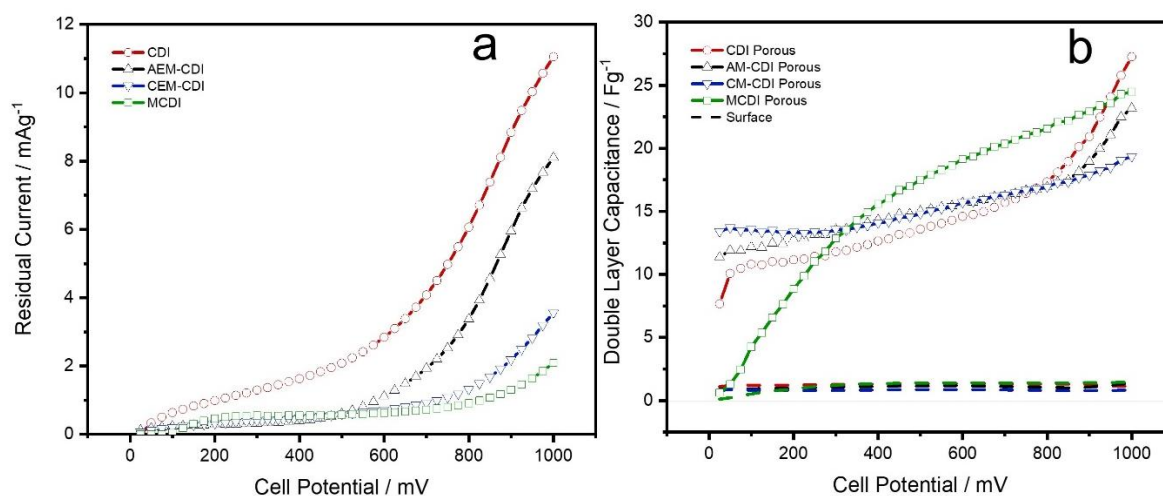
Figure 9 a) Residual current as a function of cell potential. b) specific capacitance (geometric and porous area components) as a function of potential. Geometric component is similar for all configuration, with the exception of mCDI for which it is zero.

Conclusion

Capacitive deionization is a promising desalination technology for its energy efficiency and ion selectivity. In this work, a lab-made CDI system was optimized for optimum electrochemical performance and operational stability. This is an obvious prerequisite to the operability and reliability of CDI desalination performance. Optimization is achieved by means of electrode preparation, cell set-up, the use of ionic-exchange-membranes, and defining an optimum potential window for preliminary performance tests, maintaining reasonable stable conditions, by preventing or at least reducing fast ageing of the active electrode material, namely at the positive electrode.

Electrode preparation has a significant impact on the desalination performance of CDI, particularly through the effect of pre-wetting. It is realized that soaking electrodes in 10 mM NaCl solution significantly boost the initial performance of CDI. Secondly, the extent of cell tightening has a positive correlation with the desalination performance of CDI, where the cell tightened to 150 μm free space between the cell body and cell cover shows around 30% higher SAC values than that with a 450 μm free space. Upon tightening to 150 μm free space between top and body of the cell, the effect of flowrate on desalination performance seems not to be significant .

A major challenge of CDI is operational stability and performance degradation, where the pH of the effluent varies significantly during operation, while desalination performance shows a steady decline slope starting from the first few cycles. This raises a significant challenge to utilize CDI for real life applications. However, it is realized that the major phenomenon affecting pH variations and performance degradation is the presence of faradic reactions. A direct correlation between cell potential and extent of faradic reactions is observed by means of pH fluctuations (due to acidification or alkalinization) and residual current calculations.

Faradic reactions can be suppressed to some extent by using ionic exchange membranes and optimizing the potential window. It is realized that it is best to operate with MCDI as it significantly suppresses faradic processes, at least at the cathode, while showing the highest values of columbic efficiency, lowest values for residual current, and reasonably high values of specific capacitance particularly at potentials higher than 600 mV. CEM-CDI seems to be the second-best alternative, in terms of effective limitation of faradic losses; however, the relative importance of faradic losses is not the only factor to be considered for a reliable evaluation. CDI is the most deteriorating of all configurations, showing maximal extent of acidification, highest values of residual current, and declining slope of SAC vs time, showing that it would lose around 20% of its performance after around 41 hours of operation (charging at 1000 mV for 10 minutes and discharging at 0 mV for 10 minutes consecutively).

Three zones potential window affect pH variations differently, the primary zone being 100 mV to 500 mV, intermediate zone being 600 mV to 800 mV, and the final zone being potentials higher than 800 mV. At the primary zone, minimal pH fluctuations are observed, followed by an increasing variation in the secondary zone, then an aggressive acidification at the final zone. This suggests that operating with potentials higher than 800 mV significantly affect operational stability and induces degradation in performance due to the extensive rate at which faradic reactions occur. On the contrary, operating with potentials lower than 600 mV yields relatively small values of specific capacitance, that directly affects the removal of charged ions from the salt solution. Thus, the potential window of 600 mV to 800 mV is the optimum balance between desalination performance and operational stability, though it does not appear to be a practical solution.

Therefore, by combining all metrics, activated carbon electrode-based CDI can be best utilized for brackish water desalination by optimizing preparation procedure to involve pre-wetting of the electrodes, tightening the cell to reduce its internal free volume, operating with both anionic exchange and cationic exchange membranes at potential range of 600 mV to 800 mV. This can attain prolonged operational stability and performance, while maximizing desalination performance within the safer limit.

List of Figures

References

[1]   D. Seckler, B. Randolph, U. Amarasinghe, of Water Resources Development Water Scarcity in the Twenty- first Century, Int. J. Water Resour. Dev. 15 (1999) 29–42.

[2]   S.L. Postel, Entering an era of water scarcity: The challenges ahead, Ecol. Appl. 10 (2000) 941–948. https://doi.org/10.1890/1051-0761(2000)010[0941:EAEOWS]2.0.CO;2.

[3]   S. Dahiya, B.K. Mishra, Enhancing understandability and performance of flow electrode capacitive deionisation by optimizing configurational and operational parameters: A review on recent progress, Sep. Purif. Technol. 240 (2020) 116660. https://doi.org/10.1016/j.seppur.2020.116660.

[4]   Y. Li, N. Chen, Z. Li, H. Shao, L. Qu, Frontiers of carbon materials as capacitive deionization electrodes, Dalt. Trans. 49 (2020) 5006–5014. https://doi.org/10.1039/d0dt00684j.

[5]   T. Younos, K.E. Tulou, Overview of Desalination Techniques, J. Contemp. Water Res. Educ. 132 (2009) 3–10. https://doi.org/10.1111/j.1936-704x.2005.mp132001002.x.

[6]   M. Shatat, S.B. Riffat, Water desalination technologies utilizing conventional and renewable energy sources, Int. J. Low-Carbon Technol. 9 (2014) 1–19. https://doi.org/10.1093/ijlct/cts025.

[7]   T. Peters, Membrane technology for water treatment, Chem. Eng. Technol. 33 (2010) 1233–1240. https://doi.org/10.1002/ceat.201000139.

[8]   S. Al-Amshawee, M.Y.B.M. Yunus, A.A.M. Azoddein, D.G. Hassell, I.H. Dakhil, H.A. Hasan, Electrodialysis desalination for water and wastewater: A review, Chem. Eng. J. 380 (2020) 122231. https://doi.org/10.1016/j.cej.2019.122231.

[9]   X. Zhang, K. Zuo, X. Zhang, C. Zhang, P. Liang, Selective ion separation by capacitive deionization (CDI) based technologies: A state-of-the-art review, Environ. Sci. Water Res. Technol. 6 (2020) 243–257. https://doi.org/10.1039/c9ew00835g.

[10]   W. Tang, J. Liang, D. He, J. Gong, L. Tang, Z. Liu, D. Wang, G. Zeng, Various cell architectures of capacitive deionization: Recent advances and future trends, Water Res. 150 (2019) 225–251. https://doi.org/10.1016/j.watres.2018.11.064.

[11]   C. Zhang, D. He, J. Ma, W. Tang, T.D. Waite, Faradaic reactions in capacitive deionization (CDI) - problems and possibilities: A review, Water Res. 128 (2018) 314–330. https://doi.org/10.1016/j.watres.2017.10.024.

[12]   B.E. Conway, The Double Layer at Capacitor Electrode Interfaces: Its Structure and Capacitance BT - Electrochemical Supercapacitors: Scientific Fundamentals and Technological Applications, Electrochem. Supercapacitors. (1999) 105–124. https://doi.org/10.1007/978-1-4757-3058-6_6 (accessed August 28, 2021).

[13]   B. Jia, W. Zhang, Preparation and Application of Electrodes in Capacitive Deionization (CDI): a State-of-Art Review, Nanoscale Res. Lett. 11 (2016) 1–25. https://doi.org/10.1186/s11671-016-1284-1.

[14]   M.A. Ahmed, S. Tewari, Capacitive deionization: Processes, materials and state

of the technology, J. Electroanal. Chem. 813 (2018) 178–192. https://doi.org/10.1016/j.jelechem.2018.02.024.

[15] M.A. Luciano, H. Ribeiro, G.E. Bruch, G.G. Silva, Efficiency of capacitive deionization using carbon materials based electrodes for water desalination, J. Electroanal. Chem. 859 (2020). https://doi.org/10.1016/j.jelechem.2020.113840.

[16] M. Sweetman, S. May, N. Mebberson, P. Pendleton, K. Vasilev, S. Plush, J. Hayball, Activated Carbon, Carbon Nanotubes and Graphene: Materials and Composites for Advanced Water Purification, C. 3 (2017) 18. https://doi.org/10.3390/c3020018.

[17] H. Li, L. Pan, T. Lu, Y. Zhan, C. Nie, Z. Sun, A comparative study on electrosorptive behavior of carbon nanotubes and graphene for capacitive deionization, J. Electroanal. Chem. 653 (2011) 40–44. https://doi.org/10.1016/j.jelechem.2011.01.012.

[18] M.W. Saleem, W.-S. Kim, Parameter-based performance evaluation and optimization of a capacitive deionization desalination process, (2018). https://doi.org/10.1016/j.desal.2018.02.023.

[19] Y. Qu, P.G. Campbell, L. Gu, J.M. Knipe, E. Dzenitis, J.G. Santiago, M. Stadermann, Energy consumption analysis of constant voltage and constant current operations in capacitive deionization, Desalination. 400 (2016) 18–24. https://doi.org/10.1016/j.desal.2016.09.014.

[20] M.E. Suss, S. Porada, X. Sun, P.M. Biesheuvel, J. Yoon, V. Presser, Water desalination via capacitive deionization: What is it and what can we expect from it?, Energy Environ. Sci. 8 (2015) 2296–2319. https://doi.org/10.1039/c5ee00519a.

[21] I. Cohen, E. Avraham, Y. Bouhadana, A. Soffer, D. Aurbach, The effect of the flow-regime, reversal of polarization, and oxygen on the long term stability in capacitive de-ionization processes, Electrochim. Acta. 153 (2015) 106–114. https://doi.org/10.1016/j.electacta.2014.12.007.

[22] N. Holubowitch, A. Omosebi, X. Gao, J. Landon, K. Liu, Quasi-Steady-State Polarization Reveals the Interplay of Capacitive and Faradaic Processes in Capacitive Deionization, ChemElectroChem. 4 (2017) 2404–2413. https://doi.org/10.1002/celc.201700082.

[23] Y.S. Choudhary, L. Jothi, G. Nageswaran, Electrochemical Characterization, Elsevier Inc., 2017. https://doi.org/10.1016/B978-0-323-46140-5.00002-9.

[24] B. van Limpt, Performance relations in Capacitive Deionization systems, 2010. http://edepot.wur.nl/154085.

[25] P. Galek, P. Bujewska, S. Donne, K. Fic, J. Menzel, New insight into ion dynamics in nanoporous carbon materials: An application of the step potential electrochemical spectroscopy (SPECS) technique and electrochemical dilatometry, Electrochim. Acta. 377 (2021). https://doi.org/10.1016/j.electacta.2021.138115.